A Fundamental Equation for Trifluoromethane (R-23)

Steven G. Penoncello[a)]
Center for Applied Thermodynamic Studies, College of Engineering, University of Idaho, Moscow, Idaho 83844-1011

Eric W. Lemmon
Physical and Chemical Properties Division, National Institute of Standards and Technology, 325 Broadway, Boulder, Colorado 80305-3328

Richard T Jacobsen
Idaho National Engineering and Environmental Laboratory, Idaho Falls, Idaho 83415-3790

Zhengjun Shan
Center for Applied Thermodynamic Studies, College of Engineering, University of Idaho, Moscow, Idaho 83844-1011

(Received 26 August 2002; revised manuscript received 7 January 2003; accepted 13 January 2003; published 15 August 2003)

A new formulation for the thermodynamic properties of trifluoromethane (R-23) is presented. The formulation is valid for single-phase and saturation states for temperatures from the triple point (118.02 K) to 475 K, pressures up to 120 MPa, and densities up to 24.31 mol/dm^3. The formulation includes a fundamental equation and ancillary functions for the estimation of saturation properties. The experimental data used to determine the fundamental equation included pressure–density–temperature $(p-\rho-T)$, isobaric heat capacity (c_p-p-T), isochoric heat capacity $(c_v-\rho-T)$, saturation heat capacity (c_σ), speed of sound $(w-p-T)$, and vapor pressure. A nonlinear regression algorithm was used to determine the constants and exponents of various functions within the formulation. Experimental data and values computed using the formulation are compared to verify the uncertainties in the calculated properties. The formulation presented may be used to compute densities to within ±0.1%, heat capacities to within ±0.5%, speed of sound to within ±0.5%, and vapor pressures to within ±0.2%, except near the critical point. [DOI: 10.1063/1.1559671]

Key words: caloric properties; density; equation of state; fundamental equation; HFC-23; R-23; thermodynamic properties; trifluoromethane.

Contents

List of Tables

List of Figures

a)Electronic mail: stevep@uidaho.edu

List of Symbols

Symbol	Physical quantity	Unit
a	Helmholtz energy	J/mol
c_p	Isobaric heat capacity	J/(mol·K)
c_v	Isochoric heat capacity	J/(mol·K)
c_σ	Saturated liquid heat capacity	J/(mol·K)
h	Enthalpy	J/mol
M	Molar mass	g/mol
p	Pressure	MPa
R	Molar gas constant	J/(mol·K)
s	Entropy	J/(mol·K)
T	Temperature	K
u	Internal energy	J/mol
w	Speed of sound	m/s
α	Reduced Helmholtz energy ($\alpha=a/RT$)	
δ	Reduced density ($\delta=\rho/\rho_c$)	
ρ	Molar density	mol/dm^3
τ	Inverse reduced temperature ($\tau=T_c/T$)	

Superscripts

0	Ideal gas property
r	Residual
$'$	Saturated liquid state
$''$	Saturated vapor state

Subscripts

0	Reference state property
c	Critical point property
calc	Calculated using an equation
data	Experimental value
l	Liquid property
nbp	Normal boiling point property
tp	Triple point property
v	Vapor property
σ	Saturation property

Physical Constants and Characteristic Properties of R-23

Symbol	Quantity	Value
R	Molar gas constant	8.314 472 J/(mol·K)
M	Molar mass	70.013 85 g/mol
T_c	Critical temperature	299.293 K
p_c	Critical pressure	4.832 MPa
ρ_c	Critical density	7.52 mol/dm^3
T_{tp}	Triple point temperature	118.02 K
p_{tp}	Triple point pressure	0.000 058 MPa
ρ_{tpl}	Liquid density at the triple point	24.308 mol/dm^3
T_{nbp}	Normal boiling point temperature	191.132 K
ρ_{nbpv}	Vapor density at the normal boiling point	0.0666 mol/dm^3
ρ_{nbpl}	Liquid density at the normal boiling point	20.648 mol/dm^3
T_0	Reference temperature	273.15 K
p_0	Reference pressure	0.001 MPa
h_0^0	Reference ideal gas enthalpy at T_0	26 621.5195 J/mol
s_0^0	Reference ideal gas entropy at T_0 and p_0	178.818 38 J/(mol·K)

1. Introduction

Trifluoromethane (R-23) is being considered as an alternative for R-503 (an azeotropic mixture of chlorotrifluoromethane and trifluoromethane) and R-13 (chlorotrifluoromethane) in low temperature cascade refrigeration systems and other low-temperature refrigeration applications. R-23 is chlorine free, thus it has a zero ozone depletion potential. It is also believed that R-23 has an estimated atmospheric lifetime of 280 years.

Prior to this work and that of Penoncello *et al.* (2000), the most comprehensive study on the thermodynamic properties of R-23 was done by Hou and Martin (1959). Their work included an equation of state and correlations for the vapor pressure, saturated vapor density, saturated liquid density, and isobaric ideal gas heat capacity. The formulation used an equation of state later designated as the Martin–Hou equation of state and was based on experimental data measured by Hou and Martin (1959) and other researchers.

Since the work of Hou and Martin (1959), and especially since 1970, a substantial amount of experimental data has been published for R-23. In 1999, work was undertaken at the National Institute of Standards and Technology (Magee and Duarte-Garza, 2000) to measure the properties of R-23 with uncertainties lower than those of other data available in the literature for $p-\rho-T$, isochoric heat capacity, and saturation heat capacity. In addition, vapor pressures at very low temperatures were determined from the measured heat capacity. The high accuracy data of Magee and Duarte-Garza (2000) helped determine the uncertainties in other data sets. A selected set of these new data and other data sets form the basis for the thermodynamic property formulation presented in this paper. The equation presented here supersedes the interim equation for R-23 published by Penoncello *et al.* (2000) that used preliminary uncorrected data measured by Magee and Duarte-Garza.

The available experimental data for R-23 are summarized in Table 1. Figures 1 and 2 show the distribution of the $p-\rho-T$ data on pressure-temperature and temperature-density coordinates. Figure 3 shows the available data for heat capacity and speed of sound.

2. Fixed Point Properties for R-23

Critical point values available from the literature are reported in Table 2. In this work, the critical temperature and density, which are used as reducing values in the fundamental equation, were obtained by fitting the data of Ohgaki *et al.* (1990) to a standard power-law equation for the critical region,

$$\frac{\rho_\sigma}{\rho_c}-1=N_1\left(1-\frac{T_\sigma}{T_c}\right)\pm N_2\left(1-\frac{T_\sigma}{T_c}\right)^{\beta}, \tag{1}$$

where T_σ is the saturation temperature and ρ_σ is the saturation density for the liquid or the vapor. Equation (1) is valid only in the critical region (above 297 K). The coefficients and exponent resulting from the fit of the data are $N_1=1.0721$, $N_2=2.0036$, and $\beta=0.3564$. The critical density and critical temperature were determined simultaneously with the coefficients and exponent using nonlinear fitting techniques. The resulting values, along with the critical pressure obtained from the fundamental equation, are

$$T_c=299.293\ \text{K},$$

$$\rho_c=7.52\ \text{mol/dm}^3, \tag{2}$$

and

$$p_c=4.832\ \text{MPa}.$$

These values are in agreement with, and within the experimental uncertainty of, the critical parameters reported for R-23 found in Table 2.

Magee and Duarte-Garza (2000) recently measured the triple point temperature of R-23. The reported value is 118.02 K, which has been adopted for this work. The triple point pressure was computed as 0.058 kPa using the fundamental equation.

3. Ancillary Functions for R-23

All thermodynamic properties including saturation properties can be computed from the fundamental equation. However, in the iterative solution of the fundamental equation, it is helpful to have equations that may be used to estimate saturation properties with reasonable accuracy. In most cases, ancillary equations for the saturation properties are developed from experimental data. However, in the case of R-23, the uncertainties in the experimental data were too large to enable fitting accurate equations, especially at lower pressures (below 1 atm). Therefore, values calculated using the Maxwell Equal Area Principle (equal Gibbs energies and saturation pressures) applied to the fundamental equation were used to develop the ancillary functions. For vapor pressures, the low temperature data of Magee and Duarte-Garza (2000) were also included.

The resulting ancillary equation for the vapor pressure is

$$\ln\left(\frac{p_\sigma}{p_c}\right)=\left(\frac{T_c}{T}\right)[-7.2631\theta+1.3140\theta^{1.5}-0.78507\theta^{2.4}-3.1991\theta^{3.9}]. \tag{3}$$

The equations for the saturated liquid (ρ') and vapor (ρ'') density are

$$\frac{\rho'}{\rho_c}=1+2.2636\theta^{0.37}+0.47007\theta^{0.94}+0.28660\theta^{3.1} \tag{4}$$

TABLE 1. Summary of experimental data for R-23

Author	Number of points	Temperature range (K)	Pressure range (MPa)	Density range (mol/dm^3)	AAD[a] (%)
$p-\rho-T$ data (except critical region)					
Aizpiri *et al.* (1991)	803	285–332	2.09–120	0.89–20	0.225
Belzile *et al.* (1979)	353	272–473	0.09–16.6	0.04–13.1	0.070
Geller *et al.* (1979)	70	123–296	4.5–50	10.9–24.6	0.225
Hori *et al.* (1981)	57	286–381	3.63–11.5	3.41–13.1	0.984
Hou and Martin (1959)	77	222–392	0.38–13.7	0.23–14.2	0.946
Kamiya *et al.* (1995)	77	309–350	5.77–12.8	5.71–8.92	0.292
Kryukov (1972)	16	286–296	0.07–0.11	0.03–0.05	0.972
Lange and Stein (1970)	25	243–368	0.69–4.48	0.28–2.7	0.132
Magee and Duarte-Garza (2000)	111	124–341	5.69–33.5	8.06–24.2	0.016
Rasskazov *et al.* (1975a)	222	258–393	0.57–19.2	0.24–14.8	0.119
Rasskazov *et al.* (1975b)	95	238–343	0.90–19.7	9.82–17.7	0.286
Rasskazov and Kryukov (1974)	103	243–373	0.5–5	0.16–5.22	0.659
Rubio *et al.* (1989)	1352	126–332	1.09–120	0.40–24.1	0.673
Timoshenko *et al.* (1975a)	178	243–363	0.1–3.5	0.03–2.29	0.067
Timoshenko *et al.* (1975b)	204	243–363	0.40–4.22	0.19–2.45	0.131
Wagner (1968)	84	203–353	0.17–3.34	0.1–1.35	0.551
Yokoyama and Takahashi (1997)	138	299–303	0.10–5.65	0.04–11.3	0.777
$p-\rho-T$ data (critical region)					
Aizpiri *et al.* (1991)	36	298–302	4.9–5.96	4.7–10.9	1.076
Hori *et al.* (1981)	18	298–303	4.71–5.55	5.72–9.72	0.386
Hou and Martin (1959)	8	298–303	4.71–5.34	4.83–10.6	0.711
Ohgaki *et al.* (1990)	138	298–300	4.6–5.09	4.34–10.5	0.129
Rubio *et al.* (1989)	20	299–302	4.76–5.96	4.7–10.9	0.794
Yokoyama and Takahashi (1997)	198	299–300	4.62–5.55	4–10.9	0.295
Second virial coefficients					
Belzile *et al.* (1976)	7	273–473			1.163
Bignell and Dunlop (1993)	3	289–309			2.660
Dymond and Smith (1964)	6	273–333			10.086
Hajjar and MacWood (1968)	4	313–403			53.355
Haworth and Sutton (1971)	3	298–328			8.240
Lange and Stein (1970)	4	243–368			0.656
Sutter and Cole (1967)	2	323–323			10.330
Sutter and Cole (1970)	3	323–404			0.471
Timoshenko *et al.* (1975a)	14	243–363			1.634
Vapor pressure data					
Hori *et al.* (1981)	35	244–298	1.05–4.71		0.507
Hou and Martin (1959)	47	141–298	0.002–4.73		0.366
Magee and Duarte-Garza (2000)	73	118–190	0.000 06–0.09		0.027
Ohgaki *et al.* (1990)	6	298–299	4.69–4.81		0.083
Popowicz *et al.* (1982)	90	133–199	0.00 6–0.16		0.601
Valentine *et al.* (1962)	13	145–191	0.003–0.10		1.069
Wagner (1968)	10	195–263	0.13–1.88		0.334
Saturated liquid density data					
Doering and Loeffler (1968)	24	193–293		11.7–20.6	0.575
Hori *et al.* (1981)	3	297–298		8.39–10.1	3.948
Hou and Martin (1959)	12	206–298		9.09–19.8	0.857
Ohgaki *et al.* (1990)	6	298–299		8.47–9.58	0.873
Shavandrin *et al.* (1975)	28	157–298		9.55–22.3	0.485
Shinsaka *et al.* (1985)	26	124–218		18.9–23.9	0.679
Saturated vapor density data					
Hori *et al.* (1981)	8	296–299		4.9–7.48	8.00
Ohgaki *et al.* (1990)	6	298–299		5.48–6.59	0.751
Shavandrin *et al.* (1975)	17	208–298		0.16–6.39	1.58

TABLE 1. Summary of experimental data for R-23—Continued

Author	Number of points	Temperature range (K)	Pressure range (MPa)	Density range (mol/dm^3)	AAD[a] (%)
Ideal gas heat capacity data					
Barho (1965)[c]	17	200–1000			0.771
Decker *et al.* (1951)[c]	11	100–1000			0.048
Ernst *et al.* (1997)	3	293–373			0.134
Gelles and Pitzer (1953)[c]	18	100–1500			0.182
Glockler and Edgell (1941)	7	250–400			3.779
Gruzdev and Shumskaya (1975)	17	300–460			0.284
Hou and Martin (1959)	7	139–444			0.614
Rodgers *et al.* (1974)[c]	18	100–1500			0.107
Valentine *et al.* (1962)[c]	50	15–500			0.017
Yokozeki *et al.* (1998)[c]	45	120–1000			0.792
Isobaric heat capacity data					
Ernst *et al.* (1997)	18	293–373	0.05–0.8		0.303
Gruzdev and Shumskaya (1975)	44	299–451	0.25–1.97		0.341
Takanuma *et al.* (1985)	45	252–383	0.50–3		2.944
Rasskazov *et al.* (1975c)	103	243–373	0.5–5		1.894
Valentine *et al.* (1962)	9	122–189	Sat. Liquid		0.299
Isochoric heat capacity data					
Magee and Duarte-Garza (2000)	111	124–341		8.06–24.2	0.369
Saturated heat capacity data					
Magee and Duarte-Garza (2000)	94	120–295			0.397
Speed of sound data					
Jarvis *et al.* (1996)[b]	89	294–318	0.11–5.04		0.215
Pires and Guedes (1999)	226	258–303	2.54–65.4		0.381
Scott (2002)	16	310	0.10–4.49		0.079

[a]Percent deviation in density for $p-\rho-T$ data, percent deviation in pressure for critical region $p-\rho-T$ data, for virial coefficients: difference in B (cm^3/mol).
[b]Excludes the critical region data from 4.826 to 5.111 MPa at 299.551 K.
[c]Calculated from statistical methods.

and

$$\ln\left(\frac{\rho''}{\rho_c}\right)=[-3.5136\theta^{0.43}-7.7491\theta^{1.4}-24.871\theta^{3.7}-65.637\theta^{8.0}]. \quad (5)$$

In these equations, $\theta=1-T/T_c$. The values of the critical parameters are given in the previous section. Comparisons between values calculated using these equations and saturation properties from the equation of state are discussed and shown in a subsequent section.

4. The Fundamental Equation for R-23

The fundamental equation used in this work is explicit in dimensionless Helmholtz energy. The functional form of this equation is given by

$$\frac{a(\rho,T)}{RT}=\alpha(\delta,\tau)=\alpha^0(\delta,\tau)+\alpha^r(\delta,\tau), \quad (6)$$

where a is the Helmholtz energy, $\delta=\rho/\rho_c$, $\tau=T_c/T$, and R is the molar gas constant, 8.314 472 J/(mol·K) (Mohr and Taylor, 1999). The reducing parameters, $T_c=299.293$ K and $\rho_c=7.52$ mol/dm^3, are identical to those used in the ancillary equations. The ideal gas part of the equation is given by

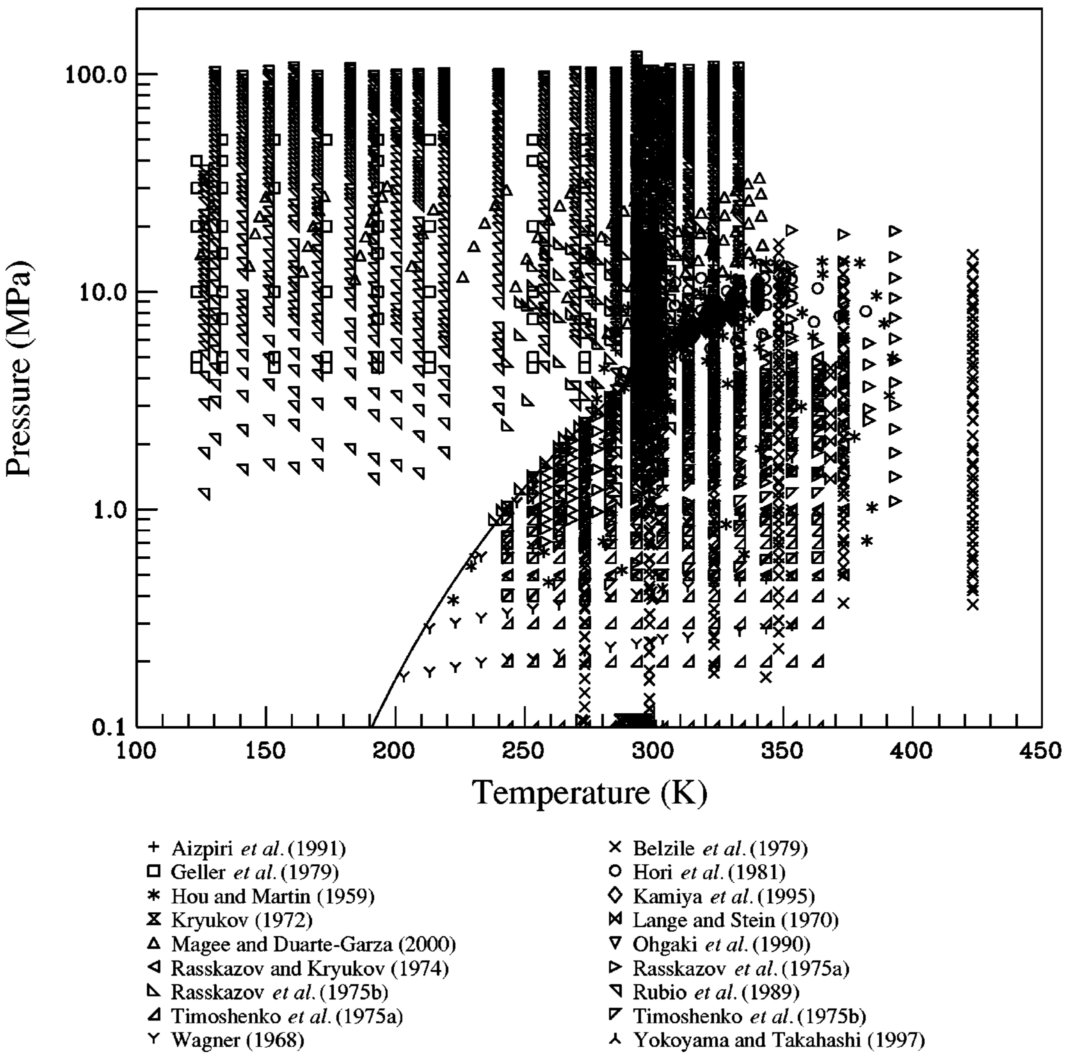

FIG. 1. Experimental $p\rho T$ data.

$$\alpha^0=\frac{h_0^0\tau}{RT_c}-\frac{s_0^0}{R}-1+\ln\frac{\delta\tau_0}{\delta_0\tau}-\frac{\tau}{R}\int_{\tau_0}^{\tau}\frac{c_p^0}{\tau^2}d\tau+\frac{1}{R}\int_{\tau_0}^{\tau}\frac{c_p^0}{\tau}d\tau, \tag{7}$$

where δ_0 is the reduced ideal gas density at $p_0=1$ kPa and $T_0=273.15$ K $[\delta_0=p_0/(\rho_c RT_0)]$, and $\tau_0=T_c/T_0$. The reference state values are $h_0^0=26\,621.5195$ J/mol and $s_0^0=178.818\,38$ J/(mol·K). These reference values of enthalpy and entropy were determined so that the saturated liquid enthalpy is 200 kJ/kg and the saturated liquid entropy is 1.0 kJ/(kg·K) at 0 °C.

The ideal gas isobaric heat capacity is given by

$$\frac{c_p^0}{R}=N_1+\sum_{i=2}^{5}N_i\frac{u_i^2\exp(u_i)}{[\exp(u_i)-1]^2}, \tag{8}$$

where $u_i=\theta_i/T$. Table 3 lists the coefficients, N_i, and the values of θ_i for this equation. The coefficients in this equation were determined simultaneously with the coefficients and exponents of the fundamental equation. Values of c_p^0 derived from statistical thermodynamics and from experimental methods, values of the speed of sound in the vapor phase, and values of the liquid isochoric heat capacity of Magee and Duarte-Garza (2000) influenced the adjustable parameters of Eq. (8). The Einstein functions containing the terms u_i were used to define the behavior of the ideal gas heat capacity consistent with that derived from statistical methods. Although the values of θ_i are of the same form as those used with wave numbers, the values given here are empirical, and the actual values of the wave numbers can be found in Rodgers *et al.* (1974). The range of validity of Eq. (8) is from 15 to 1500 K. The ideal gas Helmholtz energy equation, derived from Eqs. (7) and (8), is

$$\alpha^0=\ln\delta+a_1\ln\tau+a_2+a_3\tau+\sum_{i=4}^{7}a_i\ln[1-\exp(-b_i\tau)], \tag{9}$$

where the coefficients a_i and b_i are given in Table 4.

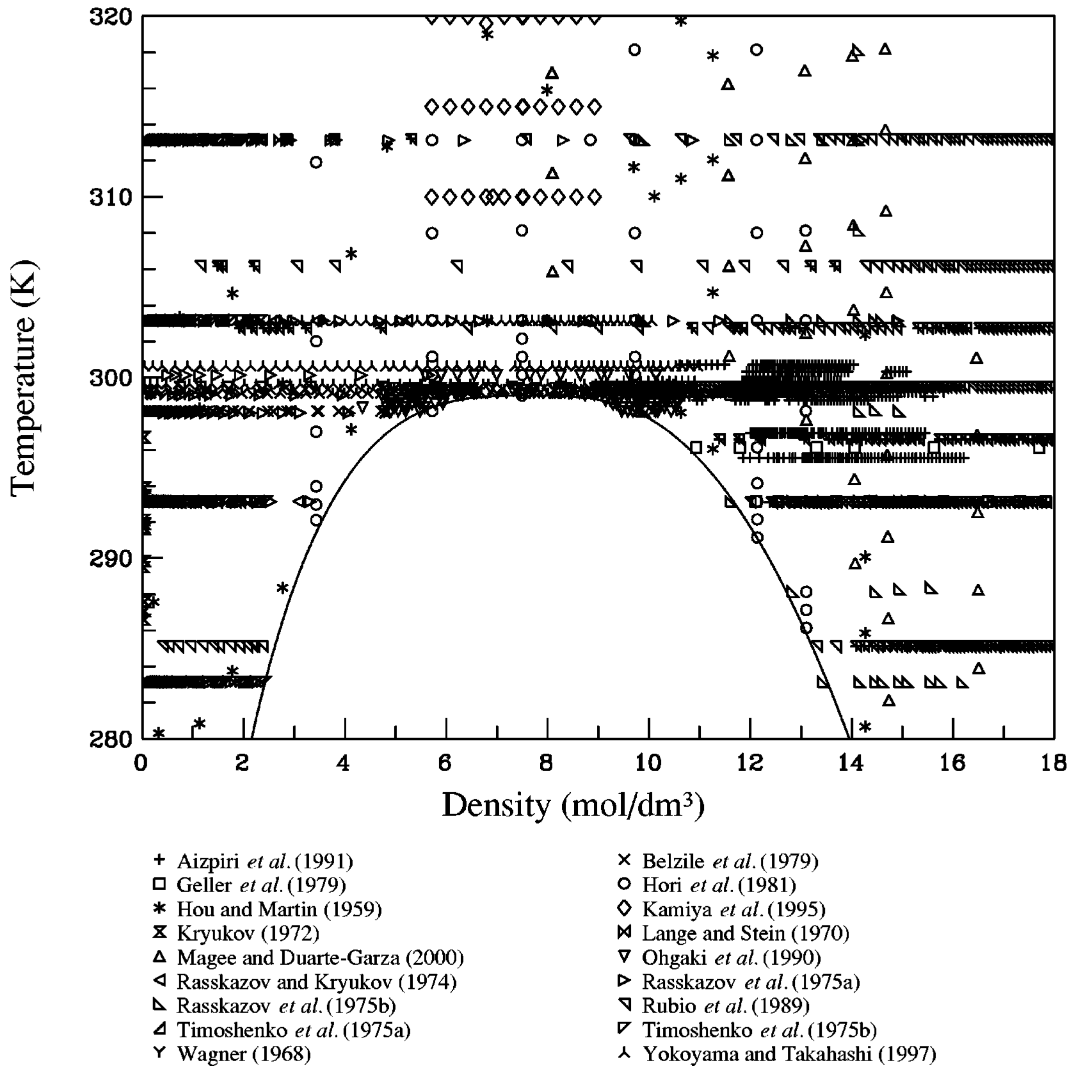

FIG. 2. Experimental $p\rho T$ data in the extended critical region.

The residual part of the dimensionless Helmholtz energy is given by

$$\alpha^r(\delta,\tau)=\sum_{k=1}^{5} N_k\delta^{i_k}\tau^{j_k}+\sum_{k=6}^{17} N_k\delta^{i_k}\tau^{j_k}\exp(-\delta^{l_k}). \tag{10}$$

The coefficients and exponents for this equation are summarized in Table 5. A nonlinear regression algorithm was used to determine the coefficients and functional form (exponents of δ and τ) of the residual dimensionless Helmholtz energy equation. Following the technique outlined in Lemmon and Jacobsen (2000), the final equation containing 17 terms was determined. The nonlinear technique simultaneously adjusted the coefficients and exponents i_k, j_k, and l_k of Eq. (10), and the coefficients of the c_p^0 function, Eq. (8). Several data forms were represented simultaneously in this process, including selected pressure–volume–temperature, heat capacity (c_v and c_p), saturated heat capacity (c_σ), speed of sound, and vapor pressure data.

4.1. Property Calculations from the Equation of State

One of the advantages of the fundamental equation explicit in Helmholtz energy is that all common thermodynamic properties are determined by differentiation. For example, the pressure derived from this form is

$$p=\rho^2\left(\frac{\partial a}{\partial \rho}\right)_T. \tag{11}$$

The equations required to calculate the derivatives needed for pressure, enthalpy, heat capacities, etc., can be found in Penoncello *et al.* (2000) or Lemmon and Jacobsen (2000). Relations for several of the most frequently calculated properties are given below:

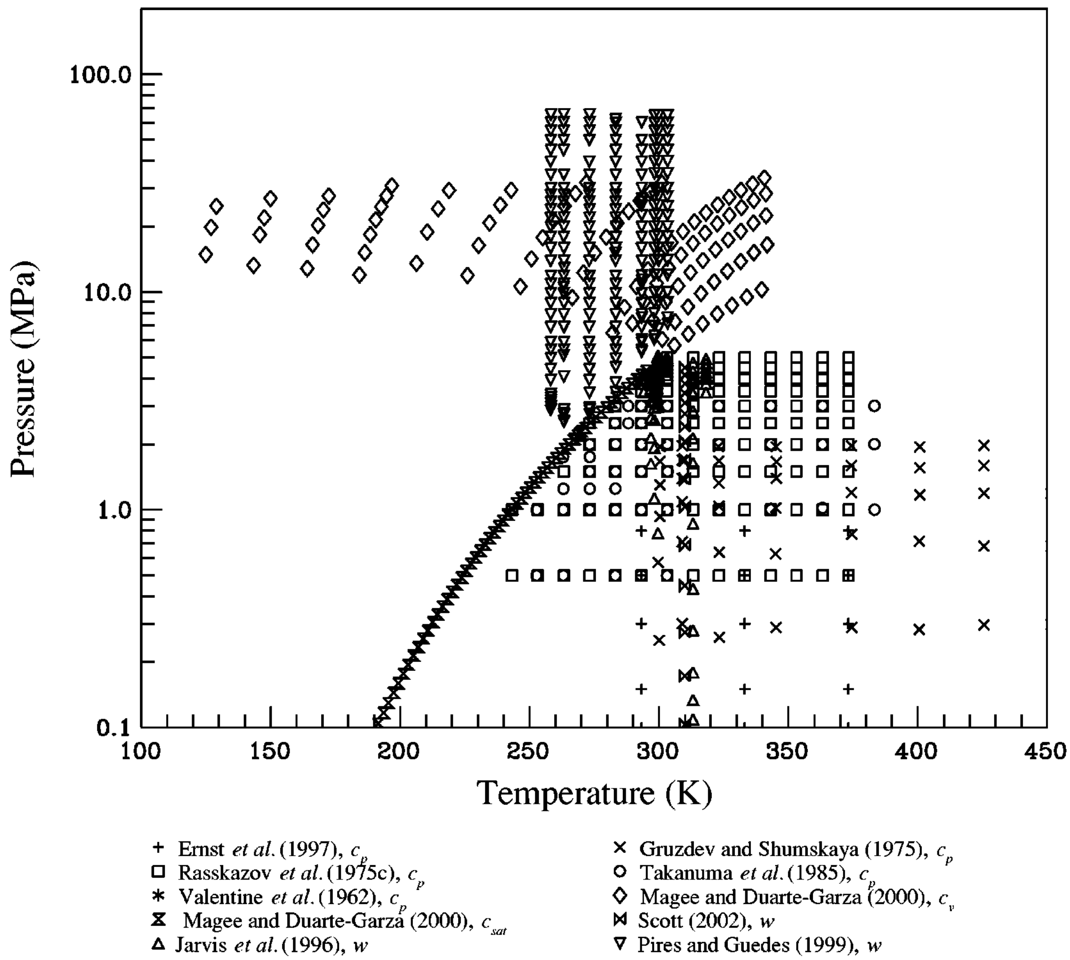

FIG. 3. Experimental heat capacity and speed of sound data.

$$p=\rho RT\left[1+\delta\left(\frac{\partial\alpha^r}{\partial\delta}\right)_\tau\right] \tag{12}$$

$$\frac{u}{RT}=\tau\left[\left(\frac{\partial\alpha^0}{\partial\tau}\right)+\left(\frac{\partial\alpha^r}{\partial\tau}\right)_\delta\right] \tag{13}$$

$$\frac{h}{RT}=\tau\left[\left(\frac{\partial\alpha^0}{\partial\tau}\right)_\delta+\left(\frac{\partial\alpha^r}{\partial\tau}\right)_\delta\right]+\delta\left(\frac{\partial\alpha^r}{\partial\delta}\right)_\tau+1 \tag{14}$$

$$\frac{s}{R}=\tau\left[\left(\frac{\partial\alpha^0}{\partial\tau}\right)_\delta+\left(\frac{\partial\alpha^r}{\partial\tau}\right)_\delta\right]-\alpha^0-\alpha^r \tag{15}$$

TABLE 2. Reported critical parameters for R-23

Author	Temperature (K)	Pressure (MPa)	Density (mol/dm^3)
Bougard and Jadot (1976)	299.05	4.863	8.121
Buchwald (1965)	298.74	4.835	7.370
Hori *et al.* (1981)	299.00	4.816	7.560
Hou and Martin (1959)	299.07	4.836	7.499
Khodeeva and Gubochkina (1977)	298.95		7.513
Kimura and Yoshimura (1992)	299.10	4.840	7.498
Ohgaki *et al.* (1990)	299.30	4.828	7.520
Platzer and Maurer (1993)	299.01	4.816	7.570
Seger (1942)	303.13		
Shavandrin *et al.* (1975)	298.97		7.506
Tsiklis and Prokhorov (1967)	299.05		7.370
Wagner (1968)	299.43	4.874	7.527
Yata *et al.* (1996)	299.06		
This work	299.293	4.832	7.52

TABLE 3. Coefficients and θ_i values of the ideal gas isobaric heat capacity equation

i	N_i	θ_i (K)
1	3.999	
2	2.371	744.0
3	3.237	1459.0
4	2.610	2135.0
5	0.8274	4911.0

$$\frac{w^2M}{RT}=1+2\delta\left(\frac{\partial\alpha^r}{\partial\delta}\right)_\tau+\delta^2\left(\frac{\partial^2\alpha^r}{\partial\delta^2}\right)_\tau-\frac{\left[1+\delta\left(\frac{\partial\alpha^r}{\partial\delta}\right)_\tau-\delta\tau\frac{\partial^2\alpha^r}{\partial\delta\partial\tau}\right]^2}{\tau^2\left[\left(\frac{\partial^2\alpha^0}{\partial\tau^2}\right)_\delta+\left(\frac{\partial^2\alpha^r}{\partial\tau^2}\right)_\delta\right]} \tag{16}$$

The derivatives of the reduced Helmholtz energy used in these relations are given in Lemmon and Jacobsen (2000).

5. Accuracy Assessment of the Equation of State for R-23

The accuracy of the fundamental equation is discussed here by comparing property values calculated with the equation of state to experimental data and by statistically analyzing the results of these comparisons. The statistics are based on the percent deviation in any property X defined as

$$\%\Delta X=100\left(\frac{X_{\text{data}}-X_{\text{calc}}}{X_{\text{data}}}\right). \tag{17}$$

Using this definition, the percent average absolute deviation (AAD) is defined as

$$\text{AAD}=\frac{1}{n}\sum_{i=1}^{n}|\%\Delta X_i|, \tag{18}$$

where n is the number of data points.

TABLE 4. Coefficients of the ideal gas Helmholtz energy equation

i	a_i	b_i
1	2.999	
2	−8.313 860 64	
3	6.550 872 53	
4	2.371	2.485 858
5	3.237	4.874 822
6	2.610	7.133 478
7	0.8274	16.408 67

TABLE 5. Coefficients and exponents of the fundamental equation

k	N_k	j_k	i_k	l_k
1	7.041 529	0.744	1	
2	−8.259 512	0.94	1	
3	0.008 053 040	4.3	1	
4	−0.086 176 15	1.46	2	
5	0.006 333 410	0.68	5	
6	−0.186 3285	4.8	1	1
7	0.328 0510	1.5	2	1
8	0.519 1023	2.07	3	1
9	0.069 161 44	0.09	5	1
10	−0.005 045 875	9.6	1	2
11	−0.017 442 21	0.19	2	2
12	−0.050 039 72	11.2	2	2
13	0.047 298 13	0.27	4	2
14	−0.061 640 31	1.6	4	2
15	0.015 835 85	10.3	4	2
16	−0.001 795 790	14.0	2	3
17	−0.001 099 007	15.0	2	4

The results of the statistical comparisons are given in Table 1. Experimental data in the critical region between 298 and 303 K at densities from 4 to 11 mol/dm^3 are not included in the first set of comparisons with $p-\rho-T$ data, but are included in the second set as deviations in pressure rather than density.

The percent deviation in thermodynamic properties computed from the fundamental equation compared to experimental data are shown in Figs. 4–7. Percent deviations of saturation properties computed from the equation of state compared to experimental data are shown in Fig. 4. Also included in Fig. 4 are percent deviations in ideal gas heat capacity calculated with the ideal gas heat capacity equation compared to experimental data.

The data available for the vapor pressure of R-23 between 210 K and the critical point are not sufficiently reliable to be used in assessing the accuracy of the equation of state. However, as shown in Fig. 4 for temperatures below 210 K, there is good agreement with the data of Magee and Duarte-Garza (2000), Popwicz *et al.* (1982) (at temperatures above 170 K), and Hou and Martin (1959) (also at temperatures above 170 K). The AAD with respect to the data sets of Magee and Duarte-Garza is 0.027%, as summarized in Table 1. During the development of the equation of state, attempts to fit the data at temperatures above 210 K caused significant deviations from other reliable data types in the same and adjacent regions of the thermodynamic surface. In the opinion of the authors, these inconsistencies with other reliable data demonstrate the higher uncertainties in the vapor pressure data from 210 K to the critical point. None of these higher temperature vapor pressure data were used to determine the final coefficients for Eqs. (6) and (10).

Figure 4 shows larger scatter for the experimental saturated liquid and vapor densities, while the values calculated from the ancillary equations are in good agreement with the

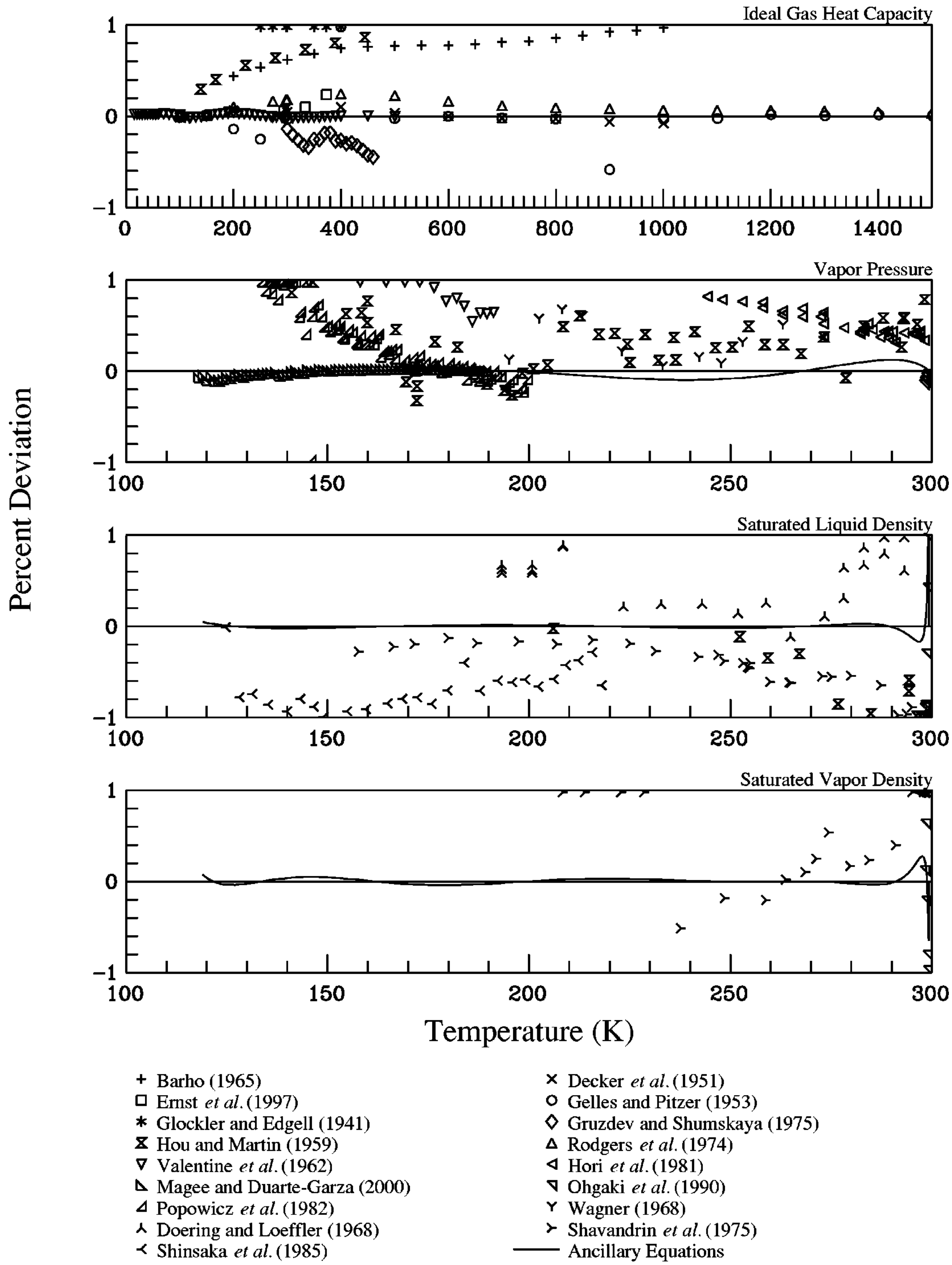

FIG. 4. Comparisons of ideal gas heat capacities, vapor pressures, and saturated liquid and vapor densities calculated with the equation of state to experimental data.

fundamental equation. None of the experimental saturation data were used in any of the fitting performed here.

Figure 5 shows the percent deviation between density values computed from the fundamental equation and the experimental $p-\rho-T$ data. There is significant scatter among the various $p-\rho-T$ data sets available for R-23. At low temperatures, the data of Rubio *et al.* (1989) differ from the data of Magee and Duarte-Garza (2000) by more than 4%. At 170 K, this difference is less than 1%. However, in these same ranges, the data of Geller *et al.* (1979) agree within 0.2% with the data of Magee and Duarte-Garza (2000). At higher temperatures, the agreement between these latter two data sets is 0.4%, but the data of Rubio *et al.* and of Magee and Duarte-Garza (2000) are quite consistent. For example, at 280 K, differences are generally less than 0.05%. In the comparisons in Fig. 5, much of the data of Rubio *et al.* [and all of the data of Aizpiri *et al.* (1991), which are identical to some of the data of Rubio *et al.*] are not shown in the comparisons

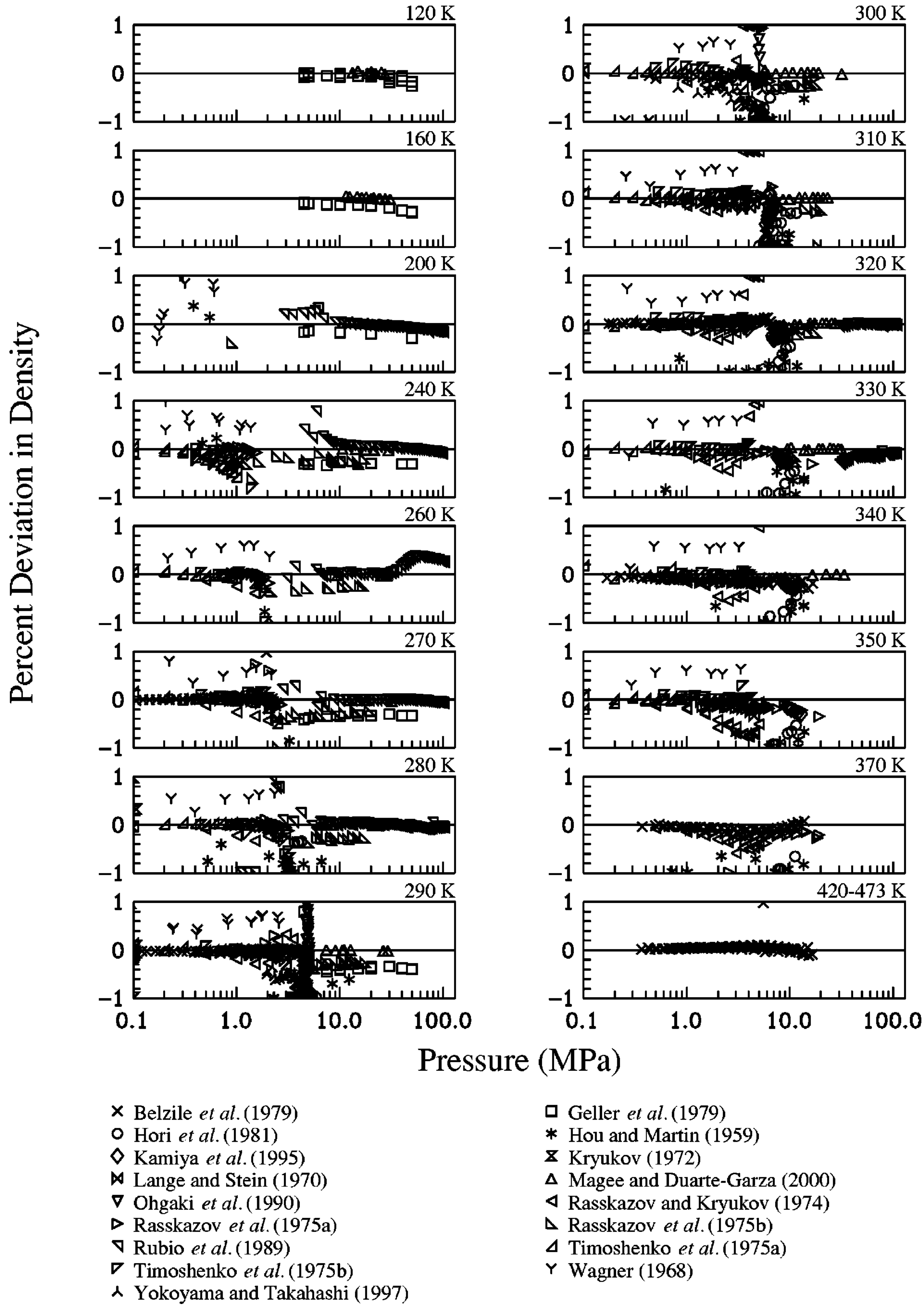

FIG. 5. Comparisons of densities calculated with the equation of state to experimental data.

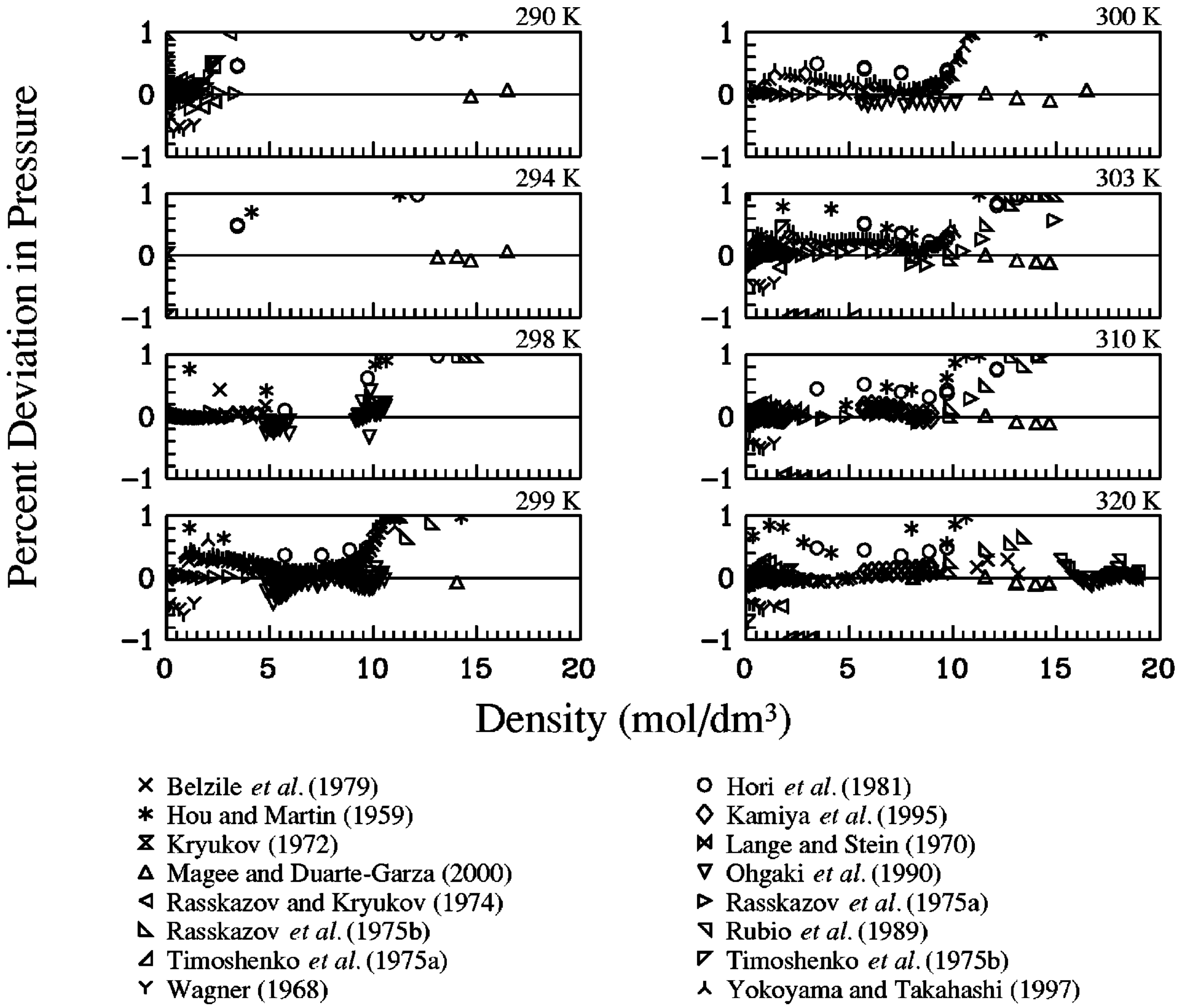

FIG. 6. Comparisons of pressures calculated with the equation of state to experimental data in the extended critical region.

since the amount of data and their higher uncertainties make it difficult to see the data of Magee and Duarte-Garza (2000). The data of Magee and Duarte-Garza (2000), which demonstrate the highest accuracy, are represented by the fundamental equation with an AAD of 0.016%.

Critical region deviations expressed as percent deviations in pressure between values computed from the equation of state and experimental $p-\rho-T$ data are shown in Fig. 6. Comparisons of the data sets in this figure also show considerable scatter. However, the calculated values exhibit good agreement with the reliable data of Magee and Duarte-Garza (2000), as previously explained. At densities less than 10 mol/dm^3 near the critical temperature, it is difficult to discern which data sets are the most accurate. Differences between the data of Ohgaki *et al.* (1990) and Yokoyama and Takahashi (1997) are about 0.3% in pressure, except very near the critical point, where the data differ by more than 1%.

Figure 7 shows the percent deviation in isobaric heat capacity, isochoric heat capacity, saturation heat capacity, and speed of sound between values computed from the equation of state and from the experimental data. For the vapor phase, the deviations between calculated isobaric heat capacities with data values between 250 and 380 K are also quite large, with many data points differing by more than 5%. However, the equation agrees well with the data of Gruzdev and Shumskaya (1975), with an AAD of 0.34%. As shown in Fig. 7, the equation is in good agreement with the vapor phase speed of sound data of Scott (2002) and Jarvis *et al.* (1996), with an AAD for each set of 0.079% and 0.21%. We conclude that the data of Gruzdev and Shumskaya are consistent with these speed of sound data and with calculated values from the fundamental equation. Comparisons in the liquid phase show deviations of less than 1% with the isobaric heat capacity data along the saturated liquid line of Valentine *et al.* (1962), and average deviations of 0.4% with the liquid phase isochoric heat capacity data of Magee and Duarte-Garza (2000). Comparisons with the saturation heat capacity data (c_σ) of Magee and Duarte-Garza (2000) are also within about 0.5%, which are lower than the reported uncertainty of the experimental data.

To ensure proper behavior of the fundamental equation, diagrams of the isochoric heat capacity, isobaric heat capac-

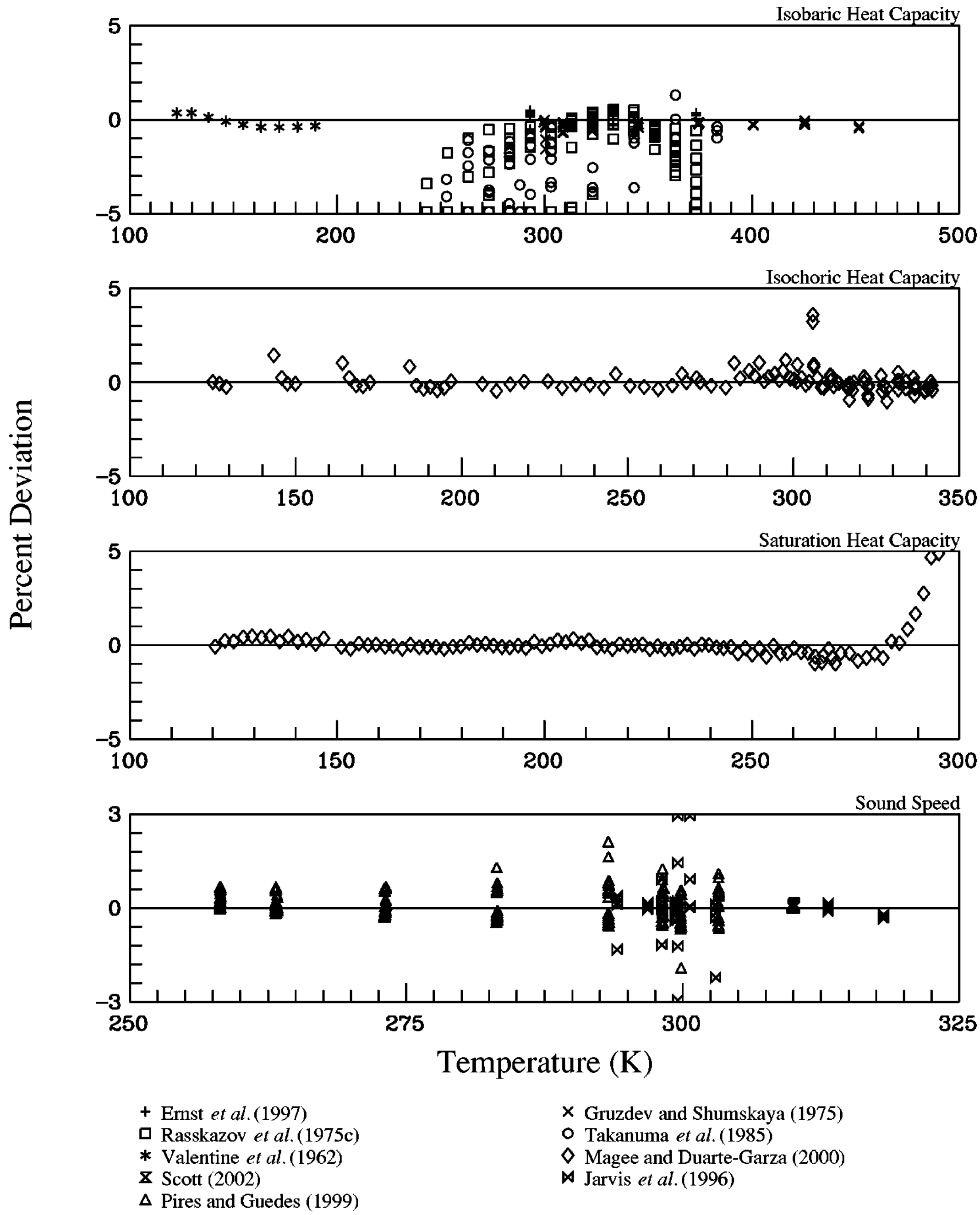

FIG. 7. Comparisons of heat capacities and speeds of sound calculated with the equation of state to experimental data.

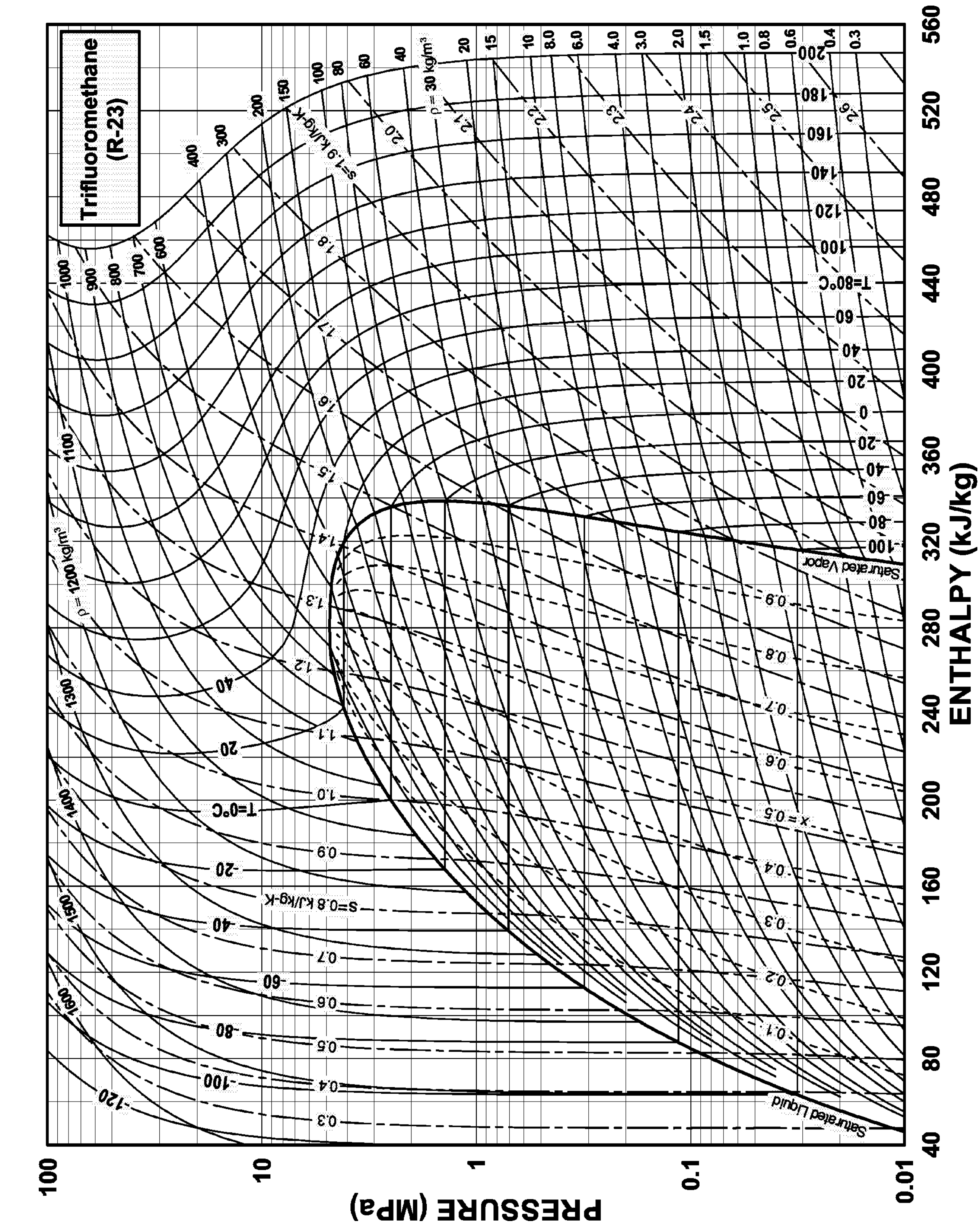

FIG. 8. Pressure versus enthalpy diagram.

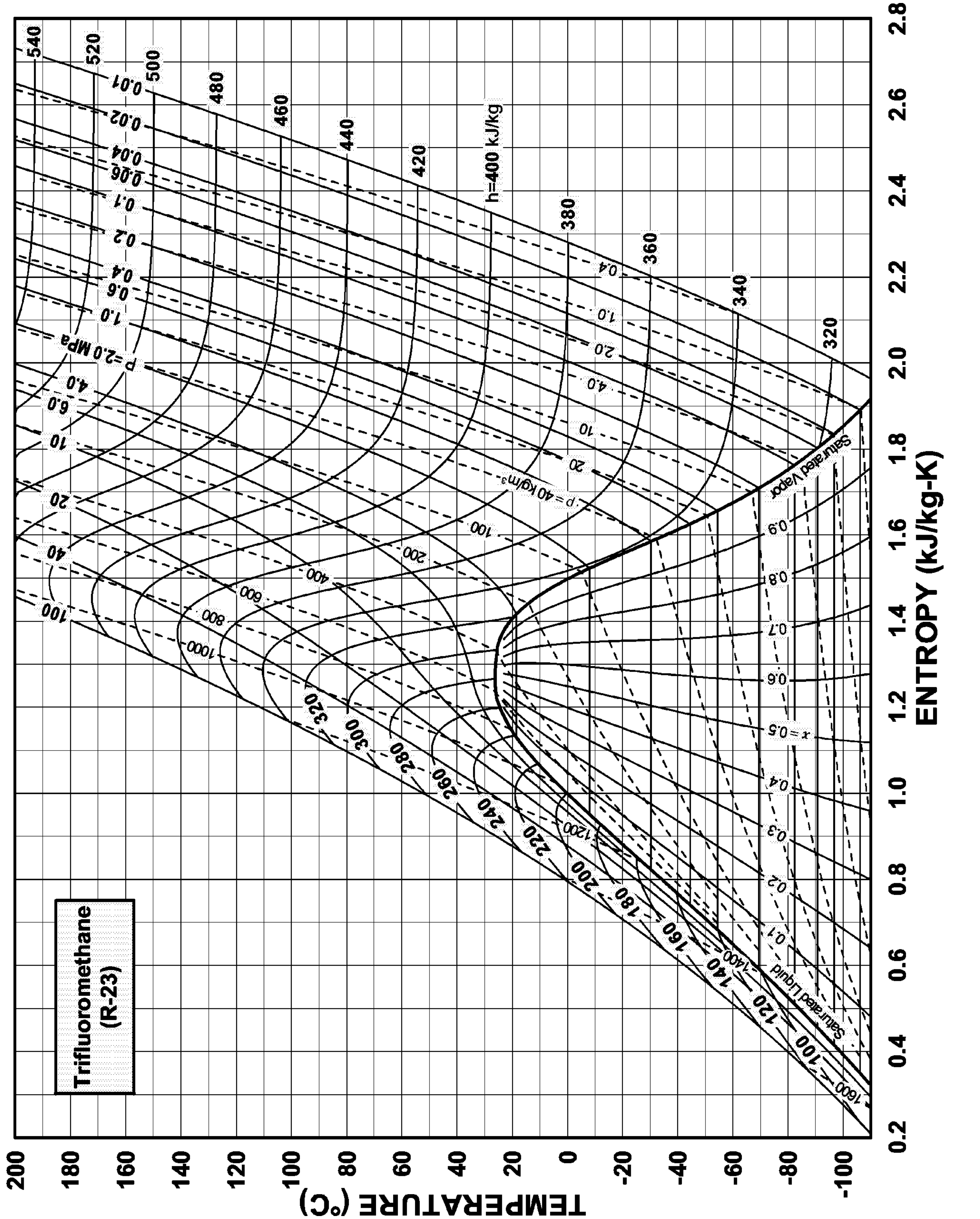

FIG. 9. Temperature versus entropy diagram.

ity, and speed of sound were made to validate the shapes of isobars over the full thermodynamic surface. The contours showed typical behavior of high accuracy fundamental equations. In addition, isotherms were drawn on a pressure–density diagram to ensure proper extrapolation behavior to high temperatures and pressures.

6. Conclusions

A fundamental equation for R-23 has been developed that is valid for temperatures from the triple point (118.02 K) to 475 K, pressures up to 120 MPa, and densities up to 24.31 mol/dm^3. The available data for $p-\rho-T$, isochoric heat capacity, saturation heat capacity, speed of sound, and vapor pressure were used simultaneously in a nonlinear regression to fit the equation. Based on the statistical and graphical analyses presented in the previous section, the fundamental equation has an estimated uncertainty of 0.1% in density, 0.5% in heat capacity, and 0.5% in speed of sound. Pressure calculations in the critical region have an estimated uncertainty of 0.2%.

An analytical equation of state cannot properly represent the nonanalytic behavior of thermodynamic properties in the critical region. Therefore, the fundamental equation reported here will not give the theoretically expected behavior for the speed of sound and heat capacities in the critical region. For R-23, the critical region is considered to be within the region bounded by $284<T<314$ K and $5.62<\rho<9.38$ mol/dm^3.

The saturation values computed from the equation of state (using the Maxwell equal area principle) have an estimated uncertainty of 0.2% in vapor pressure and saturated liquid density. The saturated vapor density uncertainty is greater than that of the saturated liquid, but is estimated to be less than 1%. To be thermodynamically consistent, saturation values should be computed from the equation of state using the Maxwell equal area principle. Values of saturation densities computed by simultaneous solution of the vapor pressure equation, Eq. (3), and the equation of state agree to within $\pm$0.1% of those calculated directly from the equation of state.

Thermodynamic properties computed using the formulation presented here are shown in the Appendix as property tables (saturation and single phase) and thermodynamic diagrams. Figure 8 is a pressure–enthalpy ($P-h$) diagram and Fig. 9 is a temperature–entropy ($T-s$) diagram for R-23.

7. Acknowledgment

The development of the preliminary fundamental equation of Penoncello *et al.* (2000), which formed the foundation of this work, was supported by the American Society of Heating, Refrigerating, and Air-conditioning Engineers (ASHRAE) under Research Project No. 997-RP.

8. References

A. G. Aizpiri, A. Rey, J. Davila, and R. G. Rubio, J. Phys. Chem. **95**, 3351 (1991).
W. Barho, Kaltetechnik **17**, 219 (1965).
J. L. Belzile, S. Kaliaguine, and R. S. Ramalho, Can. J. Chem. Eng. **54**, 446 (1976).
J. L. Belzile, S. Kaliaguine, and R. S. Ramalho, Unpublished $P-V-T$ data for R-23, National Research Council of Canada, Ottawa, Canada, 1979.
C. M. Bignell and P. J. Dunlop, J. Chem. Eng. Data **38**, 139 (1993).
J. Bougard and R. Jadot, J. Chim. Phys. **73**, 415 (1976).
H. Buchwald, Kaltetechnik **17**, 135 (1965).
C. E. Decker, A. G. Meister, and F. F. Cleveland, J. Chem. Phys. **19**, 784 (1951).
R. Doering and H. J. Loeffler, Kaltetech.-Klim. **20**, 342 (1968).
J. H. Dymond and E. B. Smith, J. Am. Chem. Soc. **60**, 1378 (1964).
G. Ernst, J. Guertner, and H. Wirbser, J. Chem. Thermodyn. **29**, 1125 (1997).
V. Z. Geller, E. G. Porichanskii, P. I. Svetlichnyi, and Yu. G. Elkin, Kholod. Tekh. Tekhnol. **29**, 43 (1979).
E. Gelles and K. S. Pitzer, J. Am. Chem. Soc. **75**, 5259 (1953).
G. Glockler and W. F. Edgell, J. Chem. Phys. **9**, 224 (1941).
V. A. Gruzdev and A. I. Shumskaya, ''Experimental Investigation of Isobaric Heat Capacity of Freons: R-11, R-12, R-13, R-21, R-22 and R-23,'' *Thermophysical Properties of Matter and Substances*, Volume 8, edited by V. A. Rabinovich (GS SSD, Moscow, 1975), pp. 108–129.
R. F. Hajjar and G. E. MacWood, J. Chem. Phys. **49**, 4567 (1968).
W. S. Haworth and L. E. Sutton, Trans. Faraday Soc. **67**, 2907 (1971).
K. Hori, S. Okazaki, M. Uematsu, and K. Watanabe, Proceedings 8th Symposium on Thermophysical Properties, New York, 1981, Vol. 2, p. 380.
Y. C. Hou and J. J. Martin, AIChE J. **5**, 125 (1959).
G. K. Jarvis, K. A. Johnson, and S. L. Walmsley, J. Chem. Eng. Data **41**, 222 (1996).
M. Kamiya, K. Muroki, and M. Uematsu, J. Chem. Thermodyn. **27**, 337 (1995).
S. M. Khodeeva and I. V. Gubochkina, Russ. J. Phys. Chem. **51**, 998 (1977).
Y. Kimura and Y. Yoshimura, J. Chem. Phys. **96**, 3085 (1992).
L. A. Kryukov, Tr. Mosk. Energ. Inst. **104**, 24 (1972).
H. B. Lange, Jr. and F. P. Stein, J. Chem. Eng. Data **15**, 56 (1970).
E. W. Lemmon and R. T Jacobsen, J. Phys. Chem. Ref. Data **29**, 521 (2000).
J. W. Magee and H. A. Duarte-Garza, Int. J. Thermophys. **21**, 1351 (2000).
P. J. Mohr and B. N. Taylor, J. Phys. Chem. Ref. Data **28**, 1713 (1999).
K. Ohgaki, S. Umezono, and T. Katayama, J. Supercritical Fluids **3**, 78 (1990).
S. G. Penoncello, Z. Shan, and R. T Jacobsen, ASHRAE Trans. **106**, 739 (2000).
P. F. Pires and H. J. R. Guedes, J. Chem. Thermodyn. **31**, 479 (1999).
B. Platzer and G. Maurer, Fluid Phase Equilib. **84**, 79 (1993).
A. Popowicz, T. Oi, J. Shulman, and T. Ishida, J. Chem. Phys. **76**, 3732 (1982).
D. S. Rasskazov and L. A. Kryukov, Tr. Mosk. Energ. Inst. **179**, 108 (1974).
D. S. Rasskazov, E. K. Petrov, G. A. Spiridonov, and E. R. Ushmaikin, Teplofiz. Svoistva Veshchestv Mater. **8**, 4 (1975a).
D. S. Rasskazov, E. K. Petrov, and E. Ushmaikin, Tr. Mosk. Energ. Inst. **234**, 52 (1975b).
D. S. Rasskazov, G. A. Spiridonov, and L. A. Krewkov, ''Experimental Investigation of Caloric Properties of Freon-23,'' *Thermophysical Properties of Matter and Substances*, Volume 8, edited by V. A. Rabinovich (GS SSD, Moscow, 1975c), pp. 100–107.
A. S. Rodgers, J. Chao, R. C. Wilhoit, and B. J. Zwolinski, J. Phys. Chem. Ref. Data **3**, 117 (1974).
R. G. Rubio, J. A. Zollweg, and W. B. Streett, Ber. Bunsenges. Phys. Chem. **93**, 791 (1989).
J. Scott (private communication, 2002, National Institute of Standards and Technology, Boulder, CO).
G. Seger, Angew. Chem. **55**, 58 (1942).
A. M. Shavandrin, T. Yu. Rasskazova, and Yu. R. Chashkin, Tr. Khim. Khim. Tekhnol. **4**, 100 (1975).
K. Shinsaka, N. Gee, and G. R. Freeman, J. Chem. Thermodyn. **17**, 1111 (1985).
H. Sutter and R. H. Cole, J. Chem. Phys. **46**, 2014 (1967).
H. Sutter and R. H. Cole, J. Chem. Phys. **52**, 132 (1970).
A. Takanuma, M. Uematsu, and K. Watanabe, Nippon Reito Kyokai Ronbunshu **2** (1985).

N. I. Timoshenko, E. P. Kholodov, and T. A. Tatarinova, Teplofiz. Svoistva Veshchestv Mater. **8**, 27 (1975a).
N. I. Timoshenko, E. P. Kholodov, and A. L. Yamnov, Teplofiz. Svoistva Veshchestv Mater. **8**, 17 (1975b).
D. S. Tsiklis and V. M. Prokhorov, Russ. J. Phys. Chem. **41**, 1182 (1967).
R. H. Valentine, G. E. Brodale, and W. F. Giauque, J. Phys. Chem. **66**, 392 (1962).
W. Wagner, Kaltetech.-Klim. **20**, 238 (1968).
J. Yata, M. Hori, H. Kawakatsu, and T. Minamiyama, Int. J. Thermophys. **17**, 65 (1996).
C. Yokoyama and M. Takahashi, Int. J. Thermophys. **18**, 1369 (1997).
A. Yokozeki, H. Sato, and K. Watanabe, Int. J. Thermophys. **19**, 89 (1998).

9. Appendix: Tables of Thermodynamic Properties of R-23

Thermodynamic properties of R-23 at saturation (at even values of temperature)

T (°C)	p (MPa)	ρ (kg/m^3)	h (kJ/kg)	s (kJ/(kg K))	c_v (kJ/(kg K))	c_p (kJ/(kg K))	w (m/s)
−155.130	0.000 06	1701.9	−3.6734	−0.070 52	0.8155	1.221	1211.2
		0.004 14	289.21	2.4111	0.3802	0.4998	135.7
−150.0	0.000 14	1685.3	2.5431	−0.018 96	0.7742	1.205	1200.1
		0.009 44	291.73	2.3293	0.3861	0.5062	138.4
−145.0	0.000 30	1668.7	8.5480	0.028 84	0.7524	1.198	1178.3
		0.019 55	294.19	2.2578	0.3927	0.5134	140.9
−140.0	0.000 60	1652.0	14.530	0.074 63	0.7399	1.195	1151.3
		0.037 98	296.65	2.1934	0.4001	0.5217	143.3
−135.0	0.001 14	1635.0	20.505	0.118 68	0.7323	1.195	1122.2
		0.069 70	299.11	2.1353	0.4083	0.5310	145.7
−130.0	0.002 06	1617.9	26.480	0.161 16	0.7274	1.195	1092.4
		0.121 66	301.56	2.0828	0.4173	0.5414	147.9
−125.0	0.003 55	1600.7	32.461	0.202 22	0.7238	1.197	1062.7
		0.203 09	304.01	2.0352	0.4269	0.5527	150.1
−120.0	0.005 88	1583.3	38.450	0.241 97	0.7212	1.199	1033.4
		0.325 78	306.45	1.9919	0.4372	0.5650	152.2
−115.0	0.009 38	1565.8	44.452	0.280 52	0.7191	1.201	1004.6
		0.504 39	308.87	1.9525	0.4482	0.5784	154.2
−110.0	0.014 47	1548.2	50.468	0.317 95	0.7175	1.205	976.2
		0.756 51	311.27	1.9165	0.4597	0.5927	156.0
−105.0	0.021 67	1530.3	56.503	0.354 36	0.7162	1.208	948.3
		1.1028	313.64	1.8836	0.4717	0.6081	157.8
−100.0	0.031 57	1512.3	62.561	0.389 82	0.7152	1.213	920.7
		1.5672	315.98	1.8534	0.4842	0.6246	159.5
−95.0	0.044 88	1494.1	68.644	0.424 40	0.7146	1.219	893.3
		2.1767	318.27	1.8256	0.4972	0.6421	161.0
−90.0	0.062 39	1475.7	74.759	0.458 19	0.7144	1.225	866.1
		2.9615	320.51	1.8000	0.5107	0.6609	162.4
−85.0	0.085 01	1456.9	80.911	0.491 24	0.7145	1.232	839.0
		3.9554	322.69	1.7763	0.5246	0.6810	163.6
−80.0	0.113 70	1437.9	87.104	0.523 63	0.7149	1.241	812.0
		5.1955	324.81	1.7543	0.5389	0.7025	164.7
−75.0	0.149 55	1418.6	93.345	0.555 40	0.7157	1.251	784.9
		6.7226	326.84	1.7338	0.5536	0.7255	165.6

Thermodynamic properties of R-23 at saturation (at even values of temperature)—Continued

T (°C)	p (MPa)	ρ (kg/m^3)	h (kJ/kg)	s (kJ/(kg K))	c_v (kJ/(kg K))	c_p (kJ/(kg K))	w (m/s)
−70.0	0.193 70	1398.9	99.641	0.586 62	0.7169	1.262	757.8
		8.5821	328.79	1.7146	0.5687	0.7501	166.3
−65.0	0.247 37	1378.7	106.00	0.617 35	0.7185	1.275	730.6
		10.824	330.65	1.6966	0.5842	0.7766	166.9
−60.0	0.311 88	1358.1	112.43	0.647 64	0.7204	1.290	703.2
		13.503	332.40	1.6796	0.6001	0.8052	167.2
−55.0	0.388 59	1337.0	118.93	0.677 54	0.7227	1.306	675.6
		16.682	334.02	1.6635	0.6163	0.8362	167.4
−50.0	0.478 93	1315.3	125.53	0.707 12	0.7254	1.325	647.9
		20.430	335.52	1.6482	0.6329	0.8701	167.3
−45.0	0.584 39	1292.9	132.22	0.736 42	0.7285	1.346	619.8
		24.830	336.86	1.6334	0.6499	0.9073	166.9
−40.0	0.706 53	1269.7	139.02	0.765 51	0.7320	1.371	591.5
		29.972	338.04	1.6191	0.6673	0.9487	166.4
−35.0	0.846 97	1245.6	145.95	0.794 45	0.7360	1.399	562.7
		35.969	339.04	1.6052	0.6852	0.9952	165.5
−30.0	1.007 39	1220.5	153.03	0.823 30	0.7405	1.432	533.6
		42.950	339.82	1.5915	0.7035	1.048	164.4
−25.0	1.189 55	1194.2	160.26	0.852 13	0.7456	1.471	504.0
		51.079	340.36	1.5779	0.7225	1.110	163.0
−20.0	1.395 29	1166.6	167.68	0.881 04	0.7514	1.517	473.8
		60.556	340.62	1.5642	0.7422	1.182	161.3
−15.0	1.626 54	1137.2	175.32	0.910 13	0.7579	1.573	443.0
		71.639	340.55	1.5502	0.7628	1.270	159.3
−10.0	1.885 35	1105.9	183.21	0.939 53	0.7654	1.643	411.4
		84.672	340.09	1.5357	0.7844	1.380	156.9
−5.0	2.173 93	1072.1	191.42	0.969 41	0.7741	1.733	378.9
		100.12	339.16	1.5204	0.8075	1.522	154.1
0.0	2.494 69	1035.1	200.00	1.0000	0.7844	1.853	345.4
		118.67	337.64	1.5039	0.8324	1.715	151.0
5.0	2.850 30	993.88	209.08	1.0317	0.7969	2.027	310.6
		141.34	335.36	1.4857	0.8596	1.995	147.3
10.0	3.243 84	946.75	218.84	1.0650	0.8128	2.300	274.1
		169.87	332.01	1.4647	0.8902	2.441	143.2
15.0	3.679 07	890.35	229.64	1.1011	0.8344	2.806	235.3
		207.58	327.06	1.4392	0.9257	3.273	138.3
20.0	4.161 03	816.43	242.36	1.1430	0.8672	4.130	192.7
		262.79	319.17	1.4050	0.9692	5.429	132.5
25.0	4.698 63	680.09	261.94	1.2067	0.9429	18.87	140.8
		379.91	301.55	1.3396	1.029	26.84	124.3
26.143	4.832 00	526.50	280.97	1.2697	1.026		122.0

Thermodynamic properties of R-23 at saturation (at even values of pressure)

T (°C)	p (MPa)	ρ (kg/m^3)	h (kJ/kg)	s (kJ/(kg K))	c_v (kJ/(kg K))	c_p (kJ/(kg K))	w (m/s)
−155.130	0.000 06	1701.9	−3.6734	−0.070 52	0.8155	1.221	1211.2
		0.004 14	289.21	2.4111	0.3802	0.4998	135.7
−147.637	0.000 2	1677.5	5.3856	0.003 90	0.7623	1.201	1190.7
		0.013 43	292.89	2.2945	0.3891	0.5095	139.6
−142.936	0.000 4	1661.9	11.019	0.047 96	0.7464	1.197	1167.6
		0.025 91	295.20	2.2304	0.3956	0.5167	141.9
−139.993	0.000 6	1652.0	14.539	0.074 69	0.7399	1.195	1151.3
		0.038 01	296.65	2.1933	0.4001	0.5217	143.3
−137.809	0.000 8	1644.6	17.149	0.094 13	0.7361	1.195	1138.7
		0.049 88	297.72	2.1672	0.4036	0.5257	144.4
−136.057	0.001	1638.6	19.242	0.109 50	0.7336	1.195	1128.4
		0.061 58	298.59	2.1471	0.4065	0.5290	145.2
−130.261	0.002	1618.8	26.168	0.158 98	0.7276	1.195	1093.9
		0.118 31	301.44	2.0854	0.4168	0.5408	147.8
−123.861	0.004	1596.8	33.824	0.211 39	0.7232	1.197	1056.0
		0.226 93	304.57	2.0250	0.4292	0.5554	150.6
−119.795	0.006	1582.6	38.696	0.243 57	0.7211	1.199	1032.2
		0.331 89	306.55	1.9902	0.4377	0.5656	152.3
−116.749	0.008	1572.0	42.351	0.267 16	0.7198	1.200	1014.6
		0.434 52	308.03	1.9659	0.4443	0.5736	153.5
−114.287	0.010	1563.3	45.309	0.285 92	0.7188	1.202	1000.5
		0.535 42	309.22	1.9472	0.4498	0.5804	154.4
−106.020	0.02	1534.0	55.270	0.347 01	0.7164	1.208	954.0
		1.0234	313.16	1.8901	0.4692	0.6049	157.5
−96.672	0.04	1500.2	66.606	0.412 93	0.7148	1.217	902.4
		1.9549	317.51	1.8347	0.4928	0.6361	160.5
−90.611	0.06	1477.9	74.011	0.454 10	0.7144	1.224	869.4
		2.8552	320.24	1.8030	0.5090	0.6586	162.2
−86.007	0.08	1460.7	79.669	0.484 65	0.7144	1.231	844.5
		3.7368	322.26	1.7809	0.5217	0.6769	163.4
−82.245	0.10	1446.5	84.318	0.509 16	0.7147	1.237	824.1
		4.6056	323.87	1.7640	0.5324	0.6927	164.2
−82.018	0.101 325	1445.6	84.599	0.510 63	0.7147	1.237	822.9
		4.6628	323.96	1.7630	0.5330	0.6936	164.3
−74.943	0.15	1418.4	93.416	0.555 76	0.7158	1.251	784.6
		6.7417	326.87	1.7336	0.5538	0.7257	165.6
−69.361	0.20	1396.3	100.45	0.590 57	0.7171	1.264	754.3
		8.8462	329.04	1.7123	0.5707	0.7534	166.4
−64.778	0.25	1377.8	106.28	0.618 70	0.7186	1.276	729.3
		10.933	330.73	1.6958	0.5849	0.7778	166.9

Thermodynamic properties of R-23 at saturation (at even values of pressure)—Continued

T (°C)	p (MPa)	ρ (kg/m^3)	h (kJ/kg)	s (kJ/(kg K))	c_v (kJ/(kg K))	c_p (kJ/(kg K))	w (m/s)
−60.857	0.30	1361.7	111.32	0.642 48	0.7200	1.287	707.9
		13.010	332.10	1.6825	0.5973	0.8001	167.2
−57.410	0.35	1347.3	115.79	0.663 17	0.7215	1.298	689.0
		15.083	333.25	1.6712	0.6085	0.8209	167.3
−54.322	0.40	1334.1	119.82	0.681 57	0.7230	1.308	671.9
		17.155	334.23	1.6614	0.6185	0.8406	167.4
−51.516	0.45	1321.9	123.52	0.698 18	0.7245	1.319	656.3
		19.229	335.08	1.6527	0.6278	0.8595	167.3
−48.938	0.50	1310.6	126.94	0.713 36	0.7260	1.329	641.9
		21.307	335.82	1.6450	0.6365	0.8777	167.2
−46.549	0.55	1299.9	130.13	0.727 37	0.7275	1.339	628.5
		23.392	336.46	1.6379	0.6446	0.8954	167.1
−44.319	0.60	1289.7	133.14	0.740 39	0.7290	1.349	616.0
		25.484	337.03	1.6314	0.6523	0.9127	166.9
−42.226	0.65	1280.1	135.98	0.752 59	0.7304	1.359	604.1
		27.585	337.54	1.6254	0.6595	0.9297	166.7
−40.250	0.70	1270.8	138.68	0.764 06	0.7318	1.369	592.9
		29.696	337.99	1.6198	0.6664	0.9465	166.4
−38.378	0.75	1262.0	141.26	0.774 91	0.7333	1.379	582.2
		31.818	338.39	1.6146	0.6730	0.9632	166.1
−36.598	0.80	1253.4	143.72	0.785 21	0.7347	1.390	572.0
		33.952	338.74	1.6096	0.6794	0.9797	165.8
−34.899	0.85	1245.1	146.10	0.795 03	0.7361	1.400	562.2
		36.099	339.05	1.6049	0.6855	0.9962	165.5
−33.274	0.90	1237.1	148.38	0.804 41	0.7375	1.410	552.7
		38.260	339.33	1.6005	0.6914	1.013	165.2
−31.715	0.95	1229.2	150.58	0.813 40	0.7389	1.420	543.7
		40.435	339.57	1.5962	0.6972	1.029	164.8
−30.217	1.00	1221.6	152.72	0.822 05	0.7403	1.430	534.9
		42.625	339.79	1.5921	0.7027	1.046	164.5
−27.380	1.10	1206.9	156.80	0.838 40	0.7431	1.451	518.2
		47.054	340.13	1.5844	0.7134	1.079	163.7
−24.731	1.20	1192.8	160.66	0.853 68	0.7459	1.473	502.4
		51.552	340.38	1.5771	0.7235	1.113	162.9
−22.242	1.30	1179.1	164.33	0.868 07	0.7487	1.495	487.4
		56.125	340.54	1.5703	0.7333	1.148	162.1
−19.892	1.40	1165.9	167.84	0.881 67	0.7515	1.518	473.1
		60.777	340.62	1.5639	0.7426	1.184	161.3
−17.665	1.50	1153.1	171.22	0.894 60	0.7543	1.541	459.5
		65.514	340.63	1.5577	0.7517	1.221	160.4

Thermodynamic properties of R-23 at saturation (at even values of pressure)—Continued

T (°C)	p (MPa)	ρ (kg/m^3)	h (kJ/kg)	s (kJ/(kg K))	c_v (kJ/(kg K))	c_p (kJ/(kg K))	w (m/s)
−15.546	1.60	1140.5	174.48	0.906 95	0.7571	1.566	446.4
		70.342	340.57	1.5517	0.7605	1.260	159.5
−13.523	1.70	1128.2	177.62	0.918 78	0.7600	1.592	433.7
		75.267	340.46	1.5460	0.7690	1.300	158.6
−11.589	1.80	1116.1	180.68	0.930 15	0.7629	1.619	421.5
		80.295	340.28	1.5404	0.7774	1.342	157.7
−7.949	2.00	1092.3	186.54	0.951 72	0.7688	1.677	398.2
		90.686	339.77	1.5295	0.7937	1.434	155.8
−4.574	2.20	1069.0	192.13	0.971 99	0.7749	1.741	376.1
		101.57	339.06	1.5190	0.8095	1.536	153.9
−1.423	2.40	1046.0	197.51	0.991 21	0.7812	1.815	355.1
		113.03	338.14	1.5088	0.8251	1.654	151.9
1.535	2.60	1022.9	202.73	1.009 6	0.7879	1.900	334.9
		125.13	337.03	1.4985	0.8404	1.789	149.9
4.323	2.80	999.76	207.82	1.027 3	0.7951	1.999	315.4
		137.98	335.72	1.4883	0.8558	1.950	147.9
6.962	3.00	976.23	212.81	1.044 5	0.8027	2.118	296.5
		151.70	334.19	1.4778	0.8712	2.143	145.8
9.467	3.20	952.13	217.76	1.061 3	0.8109	2.263	278.1
		166.47	332.43	1.4671	0.8868	2.381	143.6
11.852	3.40	927.20	222.69	1.078 0	0.8200	2.447	260.0
		182.50	330.41	1.4559	0.9027	2.683	141.5
14.128	3.60	901.10	227.65	1.094 5	0.8300	2.689	242.3
		200.10	328.08	1.4441	0.9191	3.079	139.2
16.304	3.80	873.34	232.71	1.111 3	0.8414	3.021	224.7
		219.71	325.38	1.4314	0.9361	3.626	136.9
18.387	4.00	843.21	237.94	1.128 5	0.8547	3.514	207.1
		242.04	322.20	1.4175	0.9540	4.433	134.5
20.382	4.20	809.48	243.48	1.146 6	0.8706	4.328	189.3
		268.30	318.35	1.4017	0.9731	5.747	132.0
22.295	4.40	769.69	249.60	1.166 5	0.8910	5.937	170.9
		300.92	313.48	1.3827	0.9938	8.284	129.3
24.127	4.60	717.29	257.04	1.190 7	0.9206	10.63	151.4
		346.29	306.62	1.3575	1.017	15.30	126.1
25.875	4.80	611.28	270.48	1.234 8	0.9848	93.87	128.0
		444.22	292.12	1.3071	1.040	119.1	122.0
26.143	4.8320	526.50	280.97	1.269 7	1.026		122.0

Thermodynamic properties of R-23

T (°C)	ρ (kg/m^3)	u (kJ/kg)	h (kJ/kg)	s (kJ/(kg K))	c_v (kJ/(kg K))	c_p (kJ/(kg K))	w (m/s)
				0.1 MPa			
−150.0	1685.4	2.5289	2.5882	−0.019 08	0.7741	1.205	1200.5
−140.0	1652.1	14.514	14.574	0.074 51	0.7399	1.195	1151.7
−130.0	1618.1	26.461	26.522	0.161 03	0.7274	1.195	1092.7
−120.0	1583.5	38.427	38.490	0.241 84	0.7212	1.199	1033.7
−110.0	1548.3	50.438	50.503	0.317 82	0.7175	1.204	976.6
−100.0	1512.5	62.521	62.587	0.389 71	0.7152	1.213	921.0
−90.0	1475.7	74.705	74.773	0.458 13	0.7144	1.225	866.3
−82.245	1446.5	84.248	84.318	0.509 16	0.7147	1.237	824.1
−82.245	4.6056	302.15	323.87	1.7640	0.5324	0.6927	164.2
−80.0	4.5411	303.39	325.41	1.7720	0.5277	0.6844	165.4
−70.0	4.2810	308.77	332.13	1.8059	0.5169	0.6622	170.1
−60.0	4.0558	314.05	338.70	1.8375	0.5165	0.6549	174.4
−50.0	3.8569	319.33	345.25	1.8676	0.5218	0.6558	178.5
−40.0	3.6789	324.65	351.84	1.8964	0.5304	0.6613	182.4
−30.0	3.5182	330.07	358.49	1.9244	0.5410	0.6698	186.1
−20.0	3.3720	335.58	365.24	1.9515	0.5529	0.6800	189.7
−10.0	3.2381	341.21	372.09	1.9781	0.5656	0.6915	193.2
0.0	3.1150	346.97	379.07	2.0041	0.5788	0.7038	196.5
10.0	3.0013	352.85	386.17	2.0297	0.5925	0.7166	199.8
20.0	2.8959	358.87	393.40	2.0548	0.6063	0.7299	203.1
30.0	2.7979	365.03	400.77	2.0795	0.6203	0.7433	206.2
40.0	2.7064	371.32	408.27	2.1038	0.6344	0.7569	209.3
50.0	2.6209	377.75	415.91	2.1278	0.6484	0.7706	212.3
60.0	2.5407	384.33	423.68	2.1515	0.6624	0.7843	215.3
70.0	2.4654	391.03	431.60	2.1749	0.6764	0.7980	218.2
80.0	2.3945	397.88	439.64	2.1980	0.6903	0.8116	221.1
90.0	2.3276	404.87	447.83	2.2209	0.7040	0.8251	224.0
100.0	2.2644	411.99	456.15	2.2435	0.7175	0.8385	226.8
150.0	1.9942	449.55	499.70	2.3529	0.7824	0.9027	240.3
200.0	1.7820	490.21	546.33	2.4570	0.8416	0.9615	253.0
				0.2 MPa			
−150.0	1685.5	2.5147	2.6333	−0.019 19	0.7741	1.205	1200.8
−140.0	1652.2	14.497	14.618	0.074 38	0.7400	1.195	1152.0
−130.0	1618.2	26.442	26.565	0.160 90	0.7275	1.195	1093.1
−120.0	1583.6	38.405	38.532	0.241 70	0.7213	1.198	1034.1
−110.0	1548.5	50.414	50.543	0.317 68	0.7175	1.204	977.1
−100.0	1512.7	62.493	62.626	0.389 55	0.7153	1.213	921.5
−90.0	1476.0	74.674	74.810	0.457 96	0.7144	1.225	866.9
−80.0	1438.1	86.994	87.133	0.523 47	0.7149	1.241	812.5
−70.0	1398.9	99.500	99.643	0.586 61	0.7169	1.262	757.8
−69.361	1396.3	100.31	100.45	0.590 57	0.7171	1.264	754.3
−69.361	8.8462	306.43	329.04	1.7123	0.5707	0.7534	166.4
−60.0	8.3497	311.94	335.89	1.7452	0.5515	0.7160	171.2
−50.0	7.8972	317.62	342.95	1.7775	0.5451	0.6979	175.8
−40.0	7.5030	323.23	349.89	1.8079	0.5466	0.6918	180.1
−30.0	7.1536	328.85	356.81	1.8370	0.5527	0.6928	184.1
−20.0	6.8400	334.52	363.76	1.8650	0.5616	0.6980	188.0
−10.0	6.5560	340.27	370.78	1.8922	0.5722	0.7060	191.6
0.0	6.2969	346.12	377.89	1.9187	0.5840	0.7156	195.2
10.0	6.0592	352.09	385.10	1.9446	0.5966	0.7265	198.6

Thermodynamic properties of R-23—Continued

T (°C)	ρ (kg/m^3)	u (kJ/kg)	h (kJ/kg)	s (kJ/(kg K))	c_v (kJ/(kg K))	c_p (kJ/(kg K))	w (m/s)
20.0	5.8400	358.17	392.42	1.9701	0.6097	0.7383	202.0
30.0	5.6370	364.38	399.86	1.9950	0.6231	0.7506	205.2
40.0	5.4484	370.72	407.43	2.0196	0.6367	0.7633	208.4
50.0	5.2726	377.20	415.13	2.0438	0.6504	0.7762	211.5
60.0	5.1082	383.80	422.96	2.0676	0.6641	0.7893	214.6
70.0	4.9541	390.54	430.92	2.0912	0.6779	0.8024	217.6
80.0	4.8094	397.42	439.01	2.1144	0.6915	0.8156	220.5
90.0	4.6731	404.43	447.23	2.1374	0.7051	0.8287	223.4
100.0	4.5445	411.57	455.58	2.1600	0.7185	0.8418	226.3
150.0	3.9968	449.22	499.26	2.2698	0.7830	0.9049	240.0
200.0	3.5686	489.94	545.99	2.3741	0.8420	0.9630	252.9
			0.5 MPa				
−150.0	1685.8	2.4722	2.7688	−0.019 54	0.7741	1.204	1201.9
−140.0	1652.6	14.448	14.750	0.074 01	0.7401	1.195	1153.0
−130.0	1618.6	26.386	26.695	0.160 51	0.7276	1.195	1094.1
−120.0	1584.1	38.342	38.657	0.241 28	0.7214	1.198	1035.3
−110.0	1549.0	50.342	50.665	0.317 23	0.7176	1.204	978.4
−100.0	1513.3	62.411	62.742	0.389 07	0.7153	1.212	923.0
−90.0	1476.6	74.581	74.919	0.457 44	0.7144	1.224	868.5
−80.0	1438.9	86.887	87.234	0.522 91	0.7149	1.240	814.3
−70.0	1399.8	99.376	99.733	0.585 99	0.7169	1.261	759.9
−60.0	1358.8	112.11	112.47	0.647 21	0.7203	1.288	704.7
−50.0	1315.4	125.15	125.53	0.707 06	0.7254	1.325	648.1
−48.938	1310.6	126.56	126.94	0.713 36	0.7260	1.329	641.9
−48.938	21.307	312.35	335.82	1.6450	0.6365	0.8777	167.2
−40.0	20.054	318.43	343.36	1.6780	0.6086	0.8165	172.5
−30.0	18.893	324.86	351.33	1.7114	0.5949	0.7807	177.7
−20.0	17.906	331.11	359.03	1.7425	0.5917	0.7633	182.5
−10.0	17.046	337.29	366.63	1.7719	0.5946	0.7564	186.8
0.0	16.284	343.48	374.18	1.8001	0.6011	0.7559	191.0
10.0	15.601	349.71	381.76	1.8273	0.6100	0.7595	194.9
20.0	14.982	356.01	389.38	1.8538	0.6204	0.7658	198.6
30.0	14.417	362.40	397.08	1.8796	0.6318	0.7740	202.2
40.0	13.899	368.89	404.87	1.9049	0.6439	0.7834	205.7
50.0	13.420	375.49	412.75	1.9297	0.6565	0.7938	209.1
60.0	12.977	382.21	420.74	1.9540	0.6693	0.8048	212.4
70.0	12.565	389.05	428.85	1.9780	0.6823	0.8162	215.6
80.0	12.180	396.02	437.07	2.0016	0.6954	0.8279	218.7
90.0	11.819	403.10	445.41	2.0249	0.7085	0.8398	221.8
100.0	11.481	410.31	453.87	2.0479	0.7215	0.8519	224.8
150.0	10.056	448.23	497.96	2.1587	0.7848	0.9115	239.1
200.0	8.9560	489.13	544.96	2.2636	0.8432	0.9678	252.3
			1.0 MPa				
−150.0	1686.4	2.4016	2.9946	−0.020 11	0.7740	1.204	1203.6
−140.0	1653.2	14.366	14.971	0.073 40	0.7403	1.194	1154.6
−130.0	1619.3	26.293	26.910	0.159 86	0.7279	1.194	1095.9
−120.0	1584.9	38.236	38.867	0.240 59	0.7216	1.197	1037.3
−110.0	1549.9	50.222	50.867	0.316 50	0.7178	1.203	980.6
−100.0	1514.3	62.275	62.936	0.388 29	0.7154	1.211	925.4
−90.0	1477.8	74.426	75.102	0.456 60	0.7144	1.223	871.2

Thermodynamic properties of R-23—Continued

T (°C)	ρ (kg/m^3)	u (kJ/kg)	h (kJ/kg)	s (kJ/(kg K))	c_v (kJ/(kg K))	c_p (kJ/(kg K))	w (m/s)
−80.0	1440.2	86.709	87.403	0.521 99	0.7149	1.238	817.4
−70.0	1401.3	99.170	99.883	0.584 98	0.7168	1.259	763.3
−60.0	1360.6	111.86	112.60	0.646 07	0.7201	1.286	708.5
−50.0	1317.5	124.86	125.62	0.705 77	0.7251	1.321	652.5
−40.0	1271.2	138.26	139.05	0.764 63	0.7317	1.367	594.5
−30.217	1221.6	151.90	152.72	0.822 05	0.7403	1.430	534.9
−30.217	42.625	316.33	339.79	1.5921	0.7027	1.046	164.5
−30.0	42.544	316.51	340.01	1.5930	0.7014	1.042	164.7
−20.0	39.318	324.39	349.82	1.6326	0.6606	0.9319	171.8
−10.0	36.796	331.65	358.83	1.6675	0.6420	0.8748	177.9
0.0	34.717	338.60	367.41	1.6995	0.6353	0.8442	183.3
10.0	32.945	345.40	375.76	1.7295	0.6357	0.8282	188.2
20.0	31.401	352.15	384.00	1.7581	0.6403	0.8210	192.7
30.0	30.034	358.90	392.20	1.7856	0.6476	0.8195	197.0
40.0	28.809	365.69	400.40	1.8122	0.6568	0.8218	201.1
50.0	27.701	372.54	408.64	1.8381	0.6671	0.8266	204.9
60.0	26.690	379.47	416.94	1.8634	0.6783	0.8333	208.6
70.0	25.762	386.49	425.31	1.8882	0.6900	0.8412	212.2
80.0	24.907	393.62	433.77	1.9125	0.7020	0.8501	215.7
90.0	24.114	400.84	442.31	1.9368	0.7142	0.8596	219.0
100.0	23.376	408.18	450.96	1.9598	0.7266	0.8697	222.3
150.0	20.327	446.57	495.76	2.0724	0.7878	0.9229	237.5
200.0	18.027	487.77	543.24	2.1784	0.8453	0.9758	251.5
				2.0 MPa			
−150.0	1687.4	2.2612	3.4464	−0.021 26	0.7739	1.203	1207.0
−140.0	1654.4	14.204	15.413	0.072 17	0.7408	1.193	1157.8
−130.0	1620.7	26.107	27.341	0.158 56	0.7284	1.193	1099.3
−120.0	1586.4	38.026	39.287	0.239 22	0.7221	1.196	1041.1
−110.0	1551.6	49.984	51.273	0.315 03	0.7181	1.201	984.9
−100.0	1516.2	62.006	63.325	0.386 72	0.7156	1.209	930.2
−90.0	1480.0	74.119	75.470	0.454 91	0.7146	1.220	876.6
−80.0	1442.8	86.358	87.744	0.520 16	0.7149	1.235	823.3
−70.0	1404.3	98.764	100.19	0.582 97	0.7166	1.255	770.0
−60.0	1364.1	111.39	112.86	0.643 84	0.7198	1.280	716.1
−50.0	1321.7	124.30	125.81	0.703 24	0.7245	1.313	661.1
−40.0	1276.4	137.58	139.15	0.761 69	0.7308	1.356	604.6
−30.0	1227.1	151.36	152.99	0.819 80	0.7390	1.415	545.6
−20.0	1171.9	165.82	167.53	0.878 39	0.7498	1.499	482.8
−10.0	1107.3	181.33	183.14	0.938 86	0.7648	1.636	413.6
−7.949	1092.3	184.71	186.54	0.951 72	0.7688	1.677	398.2
−7.949	90.686	317.72	339.77	1.5295	0.7937	1.434	155.8
0.0	82.728	325.97	350.14	1.5681	0.7405	1.203	164.3
10.0	75.662	334.96	361.39	1.6085	0.7065	1.063	172.7
20.0	70.337	343.18	371.62	1.6440	0.6910	0.9894	179.7
30.0	66.058	351.01	381.28	1.6765	0.6857	0.9476	185.8
40.0	62.483	358.62	390.63	1.7068	0.6864	0.9234	191.2
50.0	59.415	366.12	399.79	1.7356	0.6908	0.9097	196.3
60.0	56.733	373.59	408.84	1.7632	0.6977	0.9028	201.0
70.0	54.354	381.06	417.86	1.7898	0.7062	0.9006	205.4
80.0	52.219	388.57	426.87	1.8157	0.7158	0.9015	209.6
90.0	50.286	396.12	435.90	1.8409	0.7262	0.9047	213.6
100.0	48.524	403.75	444.97	1.8656	0.7370	0.9096	217.4

Thermodynamic properties of R-23—Continued

T (°C)	ρ (kg/m^3)	u (kJ/kg)	h (kJ/kg)	s (kJ/(kg K))	c_v (kJ/(kg K))	c_p (kJ/(kg K))	w (m/s)
150.0	41.538	443.17	491.32	1.982 1	0.7938	0.9472	234.7
200.0	36.516	485.04	539.81	2.090 4	0.8493	0.9924	249.8
			5.0 MPa				
−150.0	1690.6	1.8464	4.8039	−0.024 66	0.7739	1.199	1216.8
−140.0	1658.0	13.724	16.740	0.068 54	0.7422	1.190	1167.1
−130.0	1624.7	25.562	28.640	0.154 71	0.7300	1.190	1109.3
−120.0	1590.9	37.409	40.552	0.235 15	0.7235	1.193	1052.3
−110.0	1556.7	49.287	52.499	0.310 71	0.7192	1.197	997.4
−100.0	1522.0	61.217	64.503	0.382 12	0.7164	1.204	944.2
−90.0	1486.5	73.224	76.588	0.449 97	0.7150	1.214	892.1
−80.0	1450.3	85.338	88.785	0.514 81	0.7150	1.227	840.5
−70.0	1412.9	97.593	101.13	0.577 13	0.7164	1.244	789.1
−60.0	1374.2	110.03	113.67	0.637 38	0.7191	1.265	737.5
−50.0	1333.6	122.71	126.46	0.695 99	0.7232	1.293	685.4
−40.0	1290.8	135.68	139.55	0.753 39	0.7287	1.328	632.4
−30.0	1245.0	149.03	153.04	0.810 05	0.7356	1.373	578.1
−20.0	1195.1	162.87	167.06	0.866 51	0.7442	1.432	522.0
−10.0	1139.6	177.38	181.77	0.923 51	0.7551	1.516	463.1
0.0	1075.3	192.86	197.51	0.982 20	0.7692	1.643	400.2
10.0	995.96	209.94	214.96	1.0449	0.7897	1.876	330.0
20.0	880.89	230.65	236.33	1.1190	0.8280	2.559	244.0
30.0	327.18	302.09	317.37	1.3894	0.9549	5.652	135.3
40.0	234.45	326.18	347.50	1.4874	0.8366	2.034	155.9
50.0	201.01	339.99	364.87	1.5420	0.7929	1.529	168.1
60.0	180.45	351.29	379.00	1.5851	0.7730	1.321	177.5
70.0	165.71	361.43	391.60	1.6224	0.7646	1.210	185.4
80.0	154.29	370.94	403.35	1.6561	0.7629	1.144	192.3
90.0	145.02	380.08	414.56	1.6874	0.7652	1.102	198.4
100.0	137.25	389.00	425.43	1.7170	0.7701	1.074	204.1
150.0	110.85	432.53	477.64	1.8483	0.8118	1.032	227.5
200.0	94.698	476.69	529.49	1.9641	0.8612	1.046	246.2
			10 MPa				
−150.0	1695.8	1.1757	7.0728	−0.030 21	0.7747	1.194	1231.6
−140.0	1663.8	12.952	18.962	0.062 62	0.7451	1.186	1181.4
−130.0	1631.2	24.685	30.816	0.148 46	0.7330	1.185	1124.9
−120.0	1598.2	36.420	42.677	0.228 55	0.7261	1.187	1069.8
−110.0	1564.9	48.174	54.564	0.303 74	0.7213	1.191	1017.0
−100.0	1531.1	59.965	66.496	0.374 71	0.7180	1.196	966.0
−90.0	1496.9	71.811	78.492	0.442 07	0.7161	1.204	916.2
−80.0	1462.0	83.739	90.579	0.506 32	0.7156	1.214	867.1
−70.0	1426.2	95.774	102.79	0.567 93	0.7166	1.228	818.4
−60.0	1389.5	107.95	115.15	0.627 33	0.7188	1.245	769.9
−50.0	1351.5	120.30	127.70	0.684 87	0.7223	1.266	721.4
−40.0	1311.9	132.86	140.49	0.740 93	0.7269	1.292	672.7
−30.0	1270.4	145.69	153.56	0.795 84	0.7327	1.324	623.9
−20.0	1226.4	158.83	166.99	0.849 94	0.7397	1.362	574.6
−10.0	1179.3	172.36	180.84	0.903 61	0.7477	1.410	524.9
0.0	1128.2	186.37	195.23	0.957 27	0.7571	1.470	474.6
10.0	1071.8	200.97	210.30	1.0114	0.7680	1.548	423.7
20.0	1008.2	216.36	226.28	1.0669	0.7807	1.653	372.3

Thermodynamic properties of R-23—Continued

T (°C)	*ρ* (kg/m^3)	*u* (kJ/kg)	*h* (kJ/kg)	*s* (kJ/(kg K))	c_v (kJ/(kg K))	c_p (kJ/(kg K))	*w* (m/s)
30.0	934.62	232.81	243.51	1.1247	0.7960	1.804	320.7
40.0	846.46	250.79	262.60	1.1866	0.8145	2.030	270.5
50.0	738.67	270.87	284.40	1.2551	0.8354	2.338	226.1
60.0	616.86	292.73	308.94	1.3299	0.8504	2.513	197.3
70.0	509.41	313.63	333.27	1.4018	0.8480	2.298	187.3
80.0	432.83	331.40	354.50	1.4629	0.8367	1.955	187.7
90.0	380.34	346.37	372.67	1.5136	0.8272	1.694	191.9
100.0	342.72	359.50	388.68	1.5571	0.8223	1.521	197.2
150.0	245.06	413.75	454.55	1.7232	0.8389	1.203	223.4
200.0	199.43	462.63	512.78	1.8533	0.8792	1.142	244.9
20 MPa							
−140.0	1674.8	11.496	23.438	0.051 24	0.7516	1.178	1206.5
−130.0	1643.6	23.041	35.209	0.136 49	0.7394	1.177	1152.9
−120.0	1612.0	34.574	46.981	0.215 98	0.7316	1.178	1101.5
−110.0	1580.2	46.109	58.766	0.290 52	0.7258	1.180	1052.5
−100.0	1548.1	57.657	70.576	0.360 77	0.7216	1.183	1005.3
−90.0	1515.8	69.233	82.427	0.427 31	0.7190	1.188	959.3
−80.0	1483.1	80.853	94.338	0.490 63	0.7179	1.195	914.1
−70.0	1450.0	92.536	106.33	0.551 16	0.7183	1.204	869.6
−60.0	1416.4	104.30	118.42	0.609 27	0.7200	1.215	825.6
−50.0	1382.0	116.17	130.64	0.665 29	0.7229	1.229	782.1
−40.0	1346.9	128.17	143.02	0.719 53	0.7269	1.246	739.1
−30.0	1310.8	140.31	155.56	0.772 22	0.7319	1.264	696.7
−20.0	1273.6	152.61	168.31	0.823 60	0.7377	1.286	654.9
−10.0	1235.2	165.09	181.29	0.873 86	0.7442	1.310	613.8
0.0	1195.3	177.78	194.51	0.923 18	0.7515	1.336	573.6
10.0	1153.9	190.68	208.01	0.971 72	0.7593	1.365	534.4
20.0	1110.7	203.80	221.81	1.0196	0.7677	1.395	496.6
30.0	1065.6	217.15	235.92	1.0669	0.7764	1.428	460.4
40.0	1018.7	230.73	250.36	1.1138	0.7855	1.461	426.3
50.0	969.93	244.52	265.14	1.1603	0.7948	1.495	394.6
60.0	919.58	258.50	280.25	1.2063	0.8041	1.527	365.7
70.0	868.09	272.62	295.66	1.2519	0.8132	1.555	340.3
80.0	816.15	286.81	311.32	1.2969	0.8218	1.575	318.5
90.0	764.79	300.98	327.13	1.3410	0.8299	1.585	300.7
100.0	715.21	315.00	342.97	1.3840	0.8372	1.579	286.8
150.0	521.83	379.92	418.25	1.5736	0.8692	1.414	262.2
200.0	412.39	436.90	485.40	1.7237	0.9049	1.289	268.6
50 MPa							
−130.0	1676.7	18.814	48.635	0.104 07	0.7580	1.157	1221.6
−120.0	1648.3	29.870	60.204	0.182 18	0.7472	1.157	1180.4
−110.0	1619.9	40.902	71.768	0.255 33	0.7389	1.156	1140.8
−100.0	1591.5	51.915	83.332	0.324 12	0.7330	1.157	1102.3
−90.0	1563.2	62.915	94.902	0.389 08	0.7291	1.158	1064.3
−80.0	1534.9	73.913	106.49	0.450 68	0.7272	1.160	1026.9
−70.0	1506.7	84.916	118.10	0.509 30	0.7271	1.163	989.9
−60.0	1478.5	95.936	129.75	0.565 29	0.7284	1.168	953.6
−50.0	1450.3	106.98	141.46	0.618 95	0.7311	1.173	917.9
−40.0	1422.1	118.06	153.22	0.670 52	0.7349	1.180	883.1
−30.0	1393.9	129.19	165.06	0.720 22	0.7397	1.187	849.1

Thermodynamic properties of R-23—Continued

T (°C)	ρ (kg/m^3)	u (kJ/kg)	h (kJ/kg)	s (kJ/(kg K))	c_v (kJ/(kg K))	c_p (kJ/(kg K))	w (m/s)
−20.0	1365.7	140.36	176.97	0.768 24	0.7453	1.196	816.2
−10.0	1337.4	151.58	188.97	0.814 73	0.7516	1.204	784.3
0.0	1309.0	162.87	201.06	0.859 82	0.7585	1.214	753.6
10.0	1280.7	174.20	213.25	0.903 63	0.7660	1.223	724.2
20.0	1252.3	185.60	225.52	0.946 24	0.7739	1.233	696.1
30.0	1223.9	197.04	237.90	0.987 74	0.7821	1.242	669.3
40.0	1195.5	208.53	250.36	1.0282	0.7907	1.250	644.0
50.0	1167.3	220.07	262.90	1.0676	0.7994	1.259	620.2
60.0	1139.2	231.64	275.53	1.1061	0.8084	1.266	597.8
70.0	1111.4	243.24	288.23	1.1437	0.8175	1.273	577.0
80.0	1083.9	254.86	300.99	1.1803	0.8267	1.279	557.6
90.0	1056.7	266.49	313.81	1.2161	0.8360	1.285	539.7
100.0	1029.9	278.14	326.68	1.2511	0.8453	1.289	523.3
150.0	904.47	336.30	391.58	1.4148	0.8913	1.304	460.2
200.0	796.21	394.14	456.94	1.5608	0.9350	1.309	423.4
				100 MPa			
−120.0	1698.0	23.923	82.817	0.134 80	0.7639	1.134	1287.5
−110.0	1673.0	34.384	94.155	0.206 51	0.7538	1.134	1259.2
−100.0	1648.3	44.822	105.49	0.273 95	0.7469	1.134	1230.0
−90.0	1623.7	55.240	116.83	0.337 60	0.7429	1.133	1200.1
−80.0	1599.5	65.642	128.16	0.397 86	0.7412	1.134	1169.6
−70.0	1575.5	76.033	139.51	0.455 11	0.7414	1.135	1139.1
−60.0	1551.8	86.421	150.86	0.509 68	0.7433	1.136	1108.8
−50.0	1528.5	96.811	162.23	0.561 83	0.7465	1.139	1078.9
−40.0	1505.5	107.21	173.64	0.611 81	0.7509	1.142	1049.6
−30.0	1482.7	117.63	185.07	0.659 83	0.7563	1.145	1021.1
−20.0	1460.2	128.07	196.55	0.706 08	0.7625	1.150	993.5
−10.0	1438.1	138.53	208.07	0.750 72	0.7694	1.155	966.8
0.0	1416.1	149.03	219.64	0.793 88	0.7768	1.160	941.1
10.0	1394.5	159.56	231.27	0.835 68	0.7848	1.166	916.4
20.0	1373.1	170.13	242.95	0.876 24	0.7931	1.171	892.8
30.0	1352.0	180.73	254.70	0.915 63	0.8018	1.177	870.3
40.0	1331.2	191.38	266.50	0.953 94	0.8107	1.184	848.8
50.0	1310.7	202.07	278.37	0.991 24	0.8199	1.190	828.5
60.0	1290.5	212.80	290.30	1.0276	0.8292	1.196	809.2
70.0	1270.5	223.58	302.28	1.0630	0.8386	1.202	790.9
80.0	1250.9	234.39	314.33	1.0977	0.8482	1.208	773.6
90.0	1231.6	245.24	326.44	1.1315	0.8577	1.214	757.4
100.0	1212.6	256.14	338.60	1.1645	0.8673	1.219	742.1
150.0	1122.9	311.15	400.21	1.3194	0.9146	1.244	678.9
200.0	1042.4	367.03	462.96	1.4595	0.9594	1.265	633.7